NUREG/CR–4599
BMI–2173
Vol. 4, No. 1

Short Cracks in Piping and Piping Welds

Seventh Program Report
March 1993 – December 1994

Prepared by
G. M. Wilkowski, N. Ghadiali, D. Rudland,
P. Krishnaswamy, S. Rahman, P. Scott

Battelle

Prepared for
U.S. Nuclear Regulatory Commission

AVAILABILITY NOTICE

Availability of Reference Materials Cited in NRC Publications

Most documents cited in NRC publications will be available from one of the following sources:

1. The NRC Public Document Room, 2120 L Street, NW., Lower Level, Washington, DC 20555-0001

2. The Superintendent of Documents, U.S. Government Printing Office, P. O. Box 37082, Washington, DC 20402-9328

3. The National Technical Information Service, Springfield, VA 22161-0002

Although the listing that follows represents the majority of documents cited in NRC publications, it is not intended to be exhaustive.

Referenced documents available for inspection and copying for a fee from the NRC Public Document Room include NRC correspondence and internal NRC memoranda; NRC bulletins, circulars, information notices, inspection and investigation notices; licensee event reports; vendor reports and correspondence; Commission papers; and applicant and licensee documents and correspondence.

The following documents in the NUREG series are available for purchase from the Government Printing Office: formal NRC staff and contractor reports, NRC-sponsored conference proceedings, international agreement reports, grantee reports, and NRC booklets and brochures. Also available are regulatory guides, NRC regulations in the *Code of Federal Regulations*, and *Nuclear Regulatory Commission Issuances*.

Documents available from the National Technical Information Service include NUREG-series reports and technical reports prepared by other Federal agencies and reports prepared by the Atomic Energy Commission, forerunner agency to the Nuclear Regulatory Commission.

Documents available from public and special technical libraries include all open literature items, such as books, journal articles, and transactions. *Federal Register* notices, Federal and State legislation, and congressional reports can usually be obtained from these libraries.

Documents such as theses, dissertations, foreign reports and translations, and non-NRC conference proceedings are available for purchase from the organization sponsoring the publication cited.

Single copies of NRC draft reports are available free, to the extent of supply, upon written request to the Office of Administration, Distribution and Mail Services Section, U.S. Nuclear Regulatory Commission, Washington, DC 20555-0001.

Copies of industry codes and standards used in a substantive manner in the NRC regulatory process are maintained at the NRC Library, Two White Flint North, 11545 Rockville Pike, Rockville, MD 20852-2738, for use by the public. Codes and standards are usually copyrighted and may be purchased from the originating organization or, if they are American National Standards, from the American National Standards Institute, 1430 Broadway, New York, NY 10018-3308.

DISCLAIMER NOTICE

NUREG/CR–4599
BMI–2173
Vol. 4, No. 1

Short Cracks in Piping and Piping Welds

Seventh Program Report
March 1993 – December 1994

Manuscript Completed: January 1995
Date Published: April 1995

Prepared by
G. M. Wilkowski, N. Ghadiali, D. Rudland,
P. Krishnaswamy, S. Rahman, P. Scott

Battelle
505 King Avenue
Columbus, OH 43201

Prepared for
Division of Engineering Technology
Office of Nuclear Regulatory Research
U.S. Nuclear Regulatory Commission
Washington, DC 20555–0001
NRC Job Code B5702

ABSTRACT

This is the seventh progress report of the U.S. Nuclear Regulatory Commission's research program entitled "Short Cracks in Piping and Piping Welds". The program objective is to verify and improve fracture analyses for circumferentially cracked large-diameter nuclear piping with crack sizes typically used in leak-before-break (LBB) analyses and in-service flaw evaluations.

All work in the eight technical tasks have been completed. Ten topical reports are scheduled to be published. Progress only during the reporting period, March 1993 - December 1994, not covered in the topical reports is presented in this report.

Details about the following efforts are covered in this report:

- Improvements to the two computer programs NRCPIPE and NRCPIPES to assess the failure behavior of circumferential through-wall and surface-cracked pipe, respectively,
- Pipe material property database PIFRAC,
- Circumferentially cracked pipe database CIRCUMCK.WK1,
- An assessment of the proposed ASME Section III design stress rule changes on pipe flaw tolerance, and
- A pipe fracture experiment on a section of pipe removed from service degraded by microbiologically induced corrosion (MIC) which contained a girth weld crack.

Progress in the other tasks is not repeated here as it has been covered in great detail in the topical reports.

CONTENTS

CONTENTS

CONTENTS

Page

LIST OF TABLES

CONTENTS

Page

LIST OF FIGURES

CONTENTS

EXECUTIVE SUMMARY

The U.S. Nuclear Regulatory Commission's (NRC) "Short Cracks in Piping and Piping Welds Program" began in March of 1990 and ended in December of 1994. The program objective was to verify and improve fracture analyses for circumferentially cracked large-diameter nuclear piping using integrated results from analytical, material characterization, and full-scale pipe fracture efforts. Only quasi-static loading rates were evaluated, since the NRC's International Piping Integrity Research Group (IPIRG) Program is evaluating the effects of seismic loading rates on cracked piping systems.

The term "short cracks" encompasses crack sizes typically considered in leak-before-break (LBB) or in-service flaw evaluations. The size of a typical LBB crack for a large diameter pipe is six percent of the circumference, which is much less than the 20-to-40 percent ratios investigated in many past pipe fracture programs.

This is the seventh progress report from this program. Although termed a "semiannual report", it covers progress between March 1993 and December 1994 not presented in other topical reports that have been published in this program. There are ten topical reports that present the results from the various tasks in this program. These were published as NUREG reports by the NRC; see the list of Previous Reports in Series (page xxiii).

Progress during the reporting period, in the following six tasks, has been covered in the topical reports and is not discussed in this report.

Task 1	Through-Wall Cracked Pipe Evaluation
Task 2	Surface-Cracked Pipe Evaluation
Task 3	Bimetallic Weld Evaluation
Task 4	Dynamic Strain Aging Effects
Task 5	Anisotropy Effects
Task 6	Crack-Opening-Area Effects and Leak-Rate Quantification

Task 7 involved improving and developing the computer programs NRCPIPE and NRCPIPES used to predict load capacity and crack extension behavior for through-wall-cracked and surface-cracked pipes, respectively. Significant improvements were made to both these codes based on the analyses developed in Tasks 1 and 2. Also, the ASME Section XI flaw evaluation criteria have been included as optional analysis procedures in the NRCPIPES code. The improvements to these codes are discussed in detail in Section 2 of this report.

Task 8, Additional Efforts, produced three topical reports. A two-volume report on the "Validity of J-R Curve Limits", based on the work done by Professor Fong Shih from Brown University under a subcontract from Battelle, will also be published as a NUREG document. The other topical report in this task details the fusion-line toughness in stainless steel submerged-arc welds. Progress in compiling the pipe material property database 'PIFRAC' and the circumferentially cracked pipe fracture experiment database 'CIRCUMCK.WK1' are presented in detail in Section 3 of this report. PIFRAC contains pipe material property data. There are now 813 tensile test stress-strain curve files,

an increase from 325, and 825 J-R curve test files, an increase from 375, included in PIFRAC. CIRCUMCK.WK1 has details of over 700 pipe fracture experiments conducted throughout the world.

During this reporting period, there were two additional subtasks undertaken in Task 8. The results of those activities are reported herein. The first subtask was an assessment of how the proposed ASME Section III pipe design rule changes using elastic analyses could affect pipe flaw tolerance. The proposed changes in the design stress rules were to simplify the ASME Section III design rules and show that piping is much more forgiving than assumed by the current elastic stress analyses in the Code. Rather than to require elastic-plastic analyses, the Code Committee elected to keep the simple linear elastic analyses and, using engineering judgement and the uncracked pipe experiments as the basis, to increase the allowable stresses calculated assuming elastic conditions. There are two proposed design rule changes and the findings for them are quite different, as noted below.

The first proposed Section III design stress rule change is to increase the allowable pressure plus inertial stresses from $3S_m$ to $4.5S_m$. For this new stress level, it was shown that the ASME Section XI pipe flaw evaluation criteria (IWB-3640, IWB-3650, and Appendices C and H) would require any pipe to be repaired or replaced if the pipe had a flaw larger than the Section XI workmanship standards in Article IWB-3514. Since inertial and pressure stresses are considered as primary, or load-controlled stresses, a nonlinear correction to account for them in a simple static equivalent analysis is not technically correct. More sophisticated elastic-plastic, time-history, cracked-pipe analyses, and/or experiments would be needed to make any assessment of inertial-loaded cracked pipe at these high loads. At stresses below yield, the IPIRG-1 program results showed that inertial as well as seismic anchor motion and thermal expansion stresses act as load-controlled stresses for fracture. Furthermore, the proposed allowable stresses are twice as high as the current maximum stress in the pipe flaw evaluation criteria for a flaw that just exceeds the ASME Section XI IWB-3514 workmanship flaw limits. Hence, the tolerance of pipe with workmanship-acceptable flaws at the proposed design rule stress limits is also questionable. The EPRI/NRC Piping and Reliability program, which is the technical basis for these changes, included only experiments on uncracked pipe. None of those experiments had Code-acceptable workmanship imperfections as per Section XI Article IWB-3514. Consequently, it is not known how pipe with workmanship-acceptable flaws would behave under these high primary stresses.

The second proposed rule change is to increase the allowable stresses for secondary and pressure stresses to $7S_m$. In this case, it is technically justified to consider these stresses as displacement-controlled stresses and apply a nonlinear correction to elastic stresses to determine the actual applied moments. This was done using uncracked pipe finite element analyses with elastic and elastic-plastic analyses with Section II Code-consistent stress-strain curves for TP304 and A106 Grade B pipes. These corrected $7S_m$ moments were then used to determine the locus of critical surface-crack depths and lengths assuming limit-load failure. This locus was compared with the locus for a stress of $3S_m$. Under the restriction of displacement-controlled loading, the flaw sizes did not change significantly from $3S_m$ to $7S_m$, and they were much greater than the IWB-3514 workmanship flaw limits. An important aspect here is that this analysis was restricted to all primary stresses being below yield. However, if this second rule was implemented together with the first rule on primary stresses, then it cannot be shown that flawed pipe with any size flaw can tolerate the proposed stresses.

The second additional subtask that was added in Task 8 involved the evaluation of the fracture behavior of a microbiologically induced corrosion (MIC) defect in a pipe removed from service. This

experiment, its objectives, and the results of this evaluation are also presented in detail in Section 3. The results of this 360-degree surface-cracked pipe experiment showed that the ASME Appendix H analysis procedure (with Code default properties and an applied safety factor of 1.0) underpredicted the experimental maximum moment by a factor of three. Accounting for the actual strength, weld crown height, variability of the flaw depth, and using limit-load analyses instead of EPFM gave good agreement with the experimental moments.

ACKNOWLEDGMENTS

This work is supported by the U.S. Nuclear Regulatory Commission through the Electrical, Materials and Mechanical Engineering Branch, Division of Engineering Technology, Office of Nuclear Regulatory Research under Contract No. NRC-04-90-069. Mr. A. Hiser and Mr. M. Mayfield have been NRC program monitors.

We would like to thank those who supplied data for the pipe material property database (PIFRAC), and the pipe fracture experiment database (CIRCUMCK.WK1). The people who contributed data to the PIFRAC database were: Professor Young-Jin Kim, (Sung Kyun Kwan University - Republic of Korea), Mr. Stephen M. Graham (Materials Engineering Associates), Dr. Omeshki K. Chopra (Argonne National Laboratory), Dr. M. L. Vanderglas (Ontario Hydro - Canada), Dr. Donald McCabe (Oakridge National Laboratory), Dr. John Landes (University of Tennessee), Mr. Richard Link (Naval Surface Warfare Center), and Dr. Har Mehta (General Electric). Those that helped to supply data for the CIRCUMCK.WK1 database were: Mr. Richard Link (Naval Surface Warfare Center), Dr. Werner Stadtmüller (MPA Stuttgart - Germany), Mr. Gunther Bartholomé (Seimens/KWU - Germany), Dr. Wolfgang Brocks (Fraunhofer-Institut for Werkstoffmechanik - Germany), Dr. Claudio Maricchiolo (ANP - Italy), Dr. Katsuyuki Shibata (JAERI - Japan), Dr. Kunio Hasegawa (Hitachi - Japan), Mr. Naoki Miura (CRIEPI - Japan), Dr. Toshio Chiba (IHI - Japan), Mr. Patrick Le Delliou (EDF - France), Mr. D. Moulin (CEA - France), and Mr. Tapani Kukkola (IVO International - Finland).

We wish to thank Northeast Utilities for donating a section of pipe removed because of degradation from microbiologically induced corrosion at a girth weld and for ultrasonic inspection of the degraded area. Mr. Nelson Azevedo and Mr. Mathew Kupinski were very helpful in this effort. This pipe was used in an experiment to evaluate the accuracy of flaw evaluation criteria for such defects.

We would also like to thank others at Battelle who have helped in these efforts. Technicians who have contributed are: Mr. R. Gertler, Mr. P. Held, Mr. P. Mincer, Mr. D. Rider, and Mr. D. Shoemaker. We thank Mrs. D. Clegg, Ms. B. Fuller, Ms. A. Armitage, and Mrs. V. Kreachbaum for typing this report, and Dr. A. Hopper and Mr. K. Dufrane for editing the final draft of this document.

NOMENCLATURE

1. SYMBOLS

a	Crack length
B_1, B_2	Constants used in ASME Section III analyses
c	Half circumferential crack length
C_1	Constant in J-R curve power-law equation
d	Surface flaw depth
d_{max}	Maximum surface flaw depth
D	Nominal pipe diameter
D_i	Inside pipe diameter
D_o	Actual outside pipe diameter
I	Moment of inertia
J	J-integral fracture parameter
J_D	Deformation J
J_i	J-integral at crack initiation but not necessarily a valid J_{Ic} by ASTM E813-81
J_M	Modified value of J integral
K_r	Stress-intensity-factor to initiation-toughness ratio
m	Exponent in J-R curve power-law equation
M	Moment
n	Ramberg-Osgood strain-hardening exponent
p	Pressure
R_i	Inside pipe radius
R_m	Mean pipe radius

S_m	ASME design stress
S_r	Applied stress to limit load stress ratio in FAD
S_y	ASME yield strength
t	Thickness of pipe wall
Z	A stress multiplier in the ASME Section XI IWB-3640, IWB-3650, Appendix C, and Appendix H analyses
α	Ramberg-Osgood coefficient
β	Neutral axis angle in Net-Section-Collapse analysis
ϵ_o	Reference strain, σ_o/E
θ	Half-crack angle
σ	Stress
σ_f	Flow stress
σ_o	Reference stress (frequently equal to the yield strength)
σ_u	Ultimate stress
σ_y	Yield stress

2. ACRONYMS AND INITIALISMS

ASME	American Society of Mechanical Engineers
CEA	Commissariat a L'Energie Atomique (France)
CIRCUMCK.WK1	Lotus® database of circumferentially cracked pipe fracture experiments
CMOD	Crack-mouth-opening displacement
CRIEPI	Central Research Institute of Electric Power Industry (Japan)
C(T)	Compact (tension) specimen
d-c	Direct current

DPFAD	Deformation-plasticity failure assessment diagram
DPZP	Dimensionless plastic-zone-parameter
DTRC	David Taylor Research Center (U.S.)
EDF	Electricité de France
ENEA	Comitato Nazionale per L'Energia Nucleare e delle Energie Alternative (Italy)
EP	Electric potential
EPFM	Elastic-plastic fracture mechanics
EPRI	Electric Power Research Institute (U.S.)
FAD	Failure analysis diagram
FEM	Finite element method
GE	General Electric (U.S.)
HP	Hewlett Packard (computer)
IBM	International Business Machine (computer)
ID	Inside diameter
IPIRG	International Piping Integrity Research Group (program)
J-R	J-integral resistance (curve)
J_D-R	Deformation J-resistance (curve)
JAERI	Japanese Atomic Energy Research Institute
KWU	Kraftwerk Union Aktiengesellschaft (Germany)
LBB	Leak-before-break
LBB.ENG2	Circumferentially through-wall-cracked pipe J-estimation scheme
LBB.ENG3	Modified LBB.ENG2 method for cracks in welds
L-C	Longitudinal-circumferential orientation (direction of through-wall-crack growth around pipe circumference)

Nomenclature

LEFM	Linear elastic fracture mechanics
LVDT	Linear variable displacement transducer
MEA	Materials Engineering Associates (U.S.)
MIC	Microbiologically induced corrosion
MPA	Staatliche Materialprüfungsanstalt (University of Stuttgart, Germany)
NRC	Nuclear Regulatory Commission (U.S.)
NRCPIPE	PC computer program for circumferential TWC analyses
NRCPIPES	PC computer program for circumferential SC analyses
NSC	Net-Section-Collapse (analysis)
NUREG/CR	Nuclear Regulatory Commission Contractor Report
NUPEC	Nuclear Power Engineering Test Center (Japan)
PC	Personal computer
PIFRAC	Piping fracture database
R6	Fracture analysis methodology developed by CEGB
ROFIT	Computer code to calculate Ramberg-Osgood parameters
SAW	Submerged-arc weld
SC	Surface crack
SC.ENG	Circumferential surface-cracked pipe J-estimation analysis
SC.ENG1	Circumferential surface-cracked pipe J-estimation analysis (Method 1)
SC.ENG2	Circumferential surface-cracked pipe J-estimation analysis (Method 2)
SC.TKP	Circumferential surface-cracked pipe analysis using thick-pipe approximations
SC.TKP1	Circumferential surface-cracked pipe analysis using thick-pipe approximations and L = t

SC.TKP2	Circumferential surface-cracked pipe analysis using thick-pipe approximations and L = function of n
SC.TNP	Circumferential surface-cracked pipe analysis using thin-pipe approximations
SC.TNP1	Circumferential surface-cracked pipe analysis using thin-pipe approximations and L = t
SC.TNP2	Circumferential surface-cracked analysis using thin-pipe approximations and L = function of n
S.R.P.	Standard Review Plan
TWC	Through-wall crack, through-wall-cracked
UT	Ultrasonic testing
VAX	Mainframe computer

PREVIOUS REPORTS IN SERIES

Reports from this Program

"Short Cracks in Piping and Piping Welds," First Semiannual Report, NUREG/CR-4599, Vol. 1, No. 1, March 1991.

"Short Cracks in Piping and Piping Welds," Second Semiannual Report, NUREG/CR-4599, Vol. 1, No. 2, April 1992.

"Short Cracks in Piping and Piping Welds," Third Semiannual Report, NUREG/CR-4599, Vol. 2, No. 1, September 1992.

"Short Cracks in Piping and Piping Welds," Fourth Semiannual Report, NUREG/CR-4599, Vol. 2, No. 2, February 1993.

"Short Cracks in Piping and Piping Welds," Fifth Semiannual Report, NUREG/CR-4599, Vol. 3, No. 1, October 1993.

"Short Cracks in Piping and Piping Welds," Sixth Semiannual Report, NUREG/CR-4599, Vol. 3, No. 2, March 1994.

"Assessment of Short Through-Wall Circumferential Cracks in Pipes - Experiments and Analyses," NUREG/CR-6235, April 1995.

"Fracture Evaluations of Fusion-Line Cracks in Nuclear Pipe Bimetallic Welds," NUREG/CR-6297, April 1995.

"Effects of Toughness Anisotropy and Combined Loading on Fracture Behavior of Ferritic Nuclear Pipe," NUREG/CR-6299, April 1995.

"Dynamic Crack Instabilities in Nuclear Ferritic Piping at LWR Temperatures and the Role of Dynamic Strain Aging," NUREG/CR-6226, October 1994.

"Refinement and Evaluation of Crack-Opening Analyses for Short Circumferential Through-Wall Cracks in Pipes, " NUREG/CR-6300, April 1995.

"Probabilistic Pipe Fracture Evaluations for Leak-Rate Detection Applications," NUREG/CR-6004, April 1995.

"Validity Limits in J-Resistance Curve Determination: An Assessment of the J_M Parameter," NUREG/CR-6264, Vol. 1, February 1995.

"Validity Limits in J-Resistance Curve Determination: A Computational Approach to Ductile Crack Growth Under Large-Scale Yielding Conditions," NUREG/CR-6264, Vol. 2, February 1995.

"Stainless Steel Submerged Arc Weld Fusion Line Toughness," NUREG/CR-6251, April 1995.

Previous Related Documents from NRC's Degraded Piping Program

"Degraded Piping Program - Phase II," Semiannual Report, NUREG/CR-4082, Vol. 1, October 1984.

"Degraded Piping Program - Phase II," Semiannual Report, NUREG/CR-4082, Vol. 2, June 1985.

"Degraded Piping Program - Phase II," Semiannual Report, NUREG/CR-4082, Vol. 3, March 1986.

"Degraded Piping Program - Phase II," Semiannual Report, NUREG/CR-4082, Vol. 4, July 1986.

"Degraded Piping Program - Phase II," Semiannual Report, NUREG/CR-4082, Vol. 5, Dec. 1986.

"Degraded Piping Program - Phase II," Semiannual Report, NUREG/CR-4082, Vol. 6, April 1988.

"Degraded Piping Program - Phase II," Semiannual Report, NUREG/CR-4082, Vol. 7, March 1989.

"Degraded Piping Program - Phase II," Semiannual Report, NUREG/CR-4082, Vol. 8, March 1989.

"NRC Leak-Before-Break (LBB.NRC) Analysis Method for Circumferentially Through-Wall Cracked Pipes Under Axial Plus Bending Loads," Topical Report, NUREG/CR-4572, March 1986.

"Elastic-Plastic Finite Element Analysis of Crack Growth in Large Compact Tension and Circumferentially Through-Wall-Cracked Pipe Specimen--Results of the First Battelle/NRC Analysis Round Robin," Topical Report, NUREG/CR-4573 September 1986.

"An Experimental and Analytical Assessment of Circumferential Through-Wall Cracked Pipes Under Pure Bending," Topical Report, NUREG/CR-4574, June 1986.

"Predictions of J-R Curves With Large Crack Growth From Small Specimen Data," Topical Report, NUREG/CR-4575, August 1986.

"An Assessment of Circumferentially Complex-Cracked Pipe Subjected to Bending," Topical Report, NUREG/CR-4687, September 1986.

"Analysis of Cracks in Stainless Steel TIG Welds," Topical Report, NUREG/CR4806, Nov. 1986.

"Approximate Methods for Fracture Analyses of Through-Wall Cracked Pipes," Topical Report, NUREG/CR-4853, January 1987.

"Assessment of Design Basis for Load-Carrying Capacity of Weld-Overlay Repair," Topical Report, NUREG/CR-4877, February 1987.

"Analysis of Experiments on Stainless Steel Flux Welds," Topical Report, NUREG/CR-4878, February 1987.

"Experimental and Analytical Assessment of Circumferentially Surface-Cracked Pipes Under Bending," Topical Report, NUREG/CR-4872, April 1987.

Previous Related Documents from NRC's International Piping Integrity Research Group (IPIRG) Program

"Evaluation and Refinement of Leak-Rate Estimation Models," NUREG/CR-5128, April 1991.

"Loading Rate Effects on Strength and Fracture Toughness of Pipe Steels Used in Task 1 of the IPIRG Program," Topical Report, NUREG/CR-6098, October 1993.

1.0 INTRODUCTION

The "Short Cracks in Piping and Piping Welds" program was initiated to address Nuclear Regulatory Commission (NRC) licensing needs and to resolve some critical findings from the NRC's Degraded Piping Program. The term "short cracks" refers to the type of cracks assessed in leak-before-break (LBB) or pragmatic in-service flaw evaluations. A typical LBB-size crack for a large-diameter pipe is 6 percent of the pipe circumference, which is much less than the circumferential lengths of 20 to 40 percent investigated in other pipe fracture programs conducted in the past. Hence, the term "short cracks" in this project does not refer to microscopic cracks that are frequently of interest to the aerospace industry.

This program started on March 23, 1990. This seventh progress report describes progress in selected tasks during the period April 1993 through December 1994. Although each of the previous reports in this series covered six months of progress, this report, the last of this series, covers progress during the last 21 months of the program. During this period several topical reports covering various tasks were written. This semiannual covers only those activities not included in the topical reports. A separate final report for the entire program will also be published, which will summarize the results of the various tasks and their impact on evaluating circumferentially cracked pipe in the context of LBB and in-service flaw evaluation criteria.

The nine tasks addressed in this program are:

(1) Short through-wall-cracked (TWC) pipe evaluations
(2) Short surface-cracked (SC) pipe evaluations
(3) Bimetallic weld crack evaluations
(4) Dynamic strain aging and crack instabilities evaluations
(5) Fracture evaluations of anisotropic pipe
(6) Crack-opening-area evaluations
(7) NRCPIPE Code improvements
(8) Additional efforts
(9) Interprogram cooperation and program management.

There are ten topical reports that cover the activities in the above tasks: one for each of the first five tasks, two in Task 6, and three in Task 8.

Table 1.1 gives the updated summary of the pipe experiments conducted in this program. Most of the tasks integrate material characterization, pipe experiments, and development and improvements of analysis methods. This program addresses only circumferential cracks in straight pipe under quasi-static loading rates. Seismic loading rate and cyclic loading behavior of cracked pipe are being investigated in the NRC's Second International Piping Integrity Research Program (IPIRG-2).

Table 1.1 Matrix of pipe experiments

Experiment No.	Diameter mm (in)	Thickness mm (in)	Material	Crack Length, Percent Circumference	Crack Depth, Percent Wall Thickness	Temperature C(F)	Pressure MPa (psi)
			Uncracked Pipe Experiments				
1.1.1.25	711.0 (28.0)	24.0 (0.945)	A515 Grade 60	-0-	-0-	288 (550)	-0-
			Circumferentially Through-Wall-Cracked Experiments				
1.1.1.21	711.0 (28.0)	22.7 (0.893)	A515 Grade 60	6.25	100	288 (550)	-0-
1.1.1.23	711.0 (28.0)	30.2 (1.190)	TP316L SAW	6.25	100	288 (550)	-0-
1.1.1.24	612.0 (24.1)	31.3 (1.234)	A333 Grade 6 SAW	7.90	100	288 (550)	-0-
1.1.1.26	106.2 (4.18)	8.30 (0.327)	23 CND 18-12 (TP316L)	24.4	100	21 (70)	-0-
1.1.1.28	920.8 (36.2) 927.1 (36.5)	82.6 (3.250) 85.7 (3.380)	F316/A516 Grade 70 (Fusion line crack)	35.9	100	288 (550)	-0-
			Circumferential Surface-Cracked Pipe Experiments				
1.2.1.20	406.7 (16.0)	9.50 (0.374)	TP304	25.0	47.6	99 (210)	1.55 (225)
1.2.1.21	166.6 (6.56)	20.9 (0.822)	TP304	21.8	50.0	288 (550)	-0-
1.2.1.22	168.3 (6.64)	7.10 (0.278)	TP304	25.0	50.0	288 (550)	-0-
1.2.3.15	711.0 (28.0)	22.7 (0.893)	A515 Grade 60	25.0	50.0	288 (550)	9.56 (1387)
1.2.3.16	711.0 (28.0)	30.2 (1.190)	TP316L SAW	25.0	50.0	288 (550)	10.1 (1470)
1.2.3.17	610.0 (24.0)	42.7 (1.680)	A106B SAW	25.0	60.5	288 (550)	15.5 (2250)
1.2.3.21	168.3 (6.62)	6.35 (0.250)	A53 SMAW	100	7.0 to 63.5	23 (73)	0.70 (100)

2.0 TASK 7 NRCPIPE

2.1 Task Objective

The main objective of this task is to incorporate the analysis improvements from Tasks 1 and 2 into the NRCPIPE code. A secondary objective is to make the NRCPIPE code more efficient and also to restructure the code to allow for ease of implementation of the activities described below.

2.2 Task Rationale

In the Degraded Piping Program, the computer code NRCPIPE was developed for circumferential through-wall-cracked pipe fracture analyses. A VAX version of the code also contained the circumferential internal-surface-cracked pipe J-estimation schemes. As part of the Short Cracks in Piping and Piping Welds program, a PC version was made specifically for the through-wall-cracked pipe analyses. In addition, numerous J-estimation schemes were developed or modified. The improvements developed in the current program needed to be incorporated into this code to take advantage of technology developments as well as to facilitate comparisons with the experimental results.

2.3 Task Approach

The progress in each of these subtasks is discussed below.

Subtask 7.1 Improve Efficiency of Current Version of NRCPIPE
Subtask 7.2 TWC Improvement
Subtask 7.3 Surface Crack Code
Subtask 7.4 User's Manual

Subtask 7.1 has been completed. Progress in the remaining subtasks is detailed below.

2.3.1 Summary of Capabilities and Improvements to NRCPIPE

A revised version of the NRCPIPE code (Version 2.0) was developed during this reporting period. This section of the report summarizes the significant improvements made and the new capabilities added to the NRCPIPE Code.

User-Friendly Improvements:

- The output file includes a problem title and the version number of the code.

- Information regarding limitations and definition of certain terms were put on interactive screens.

J-estimation Capabilities and Improvements:

- The new GE/EPRI h and F functions, developed in Task 1 for bending and bending plus pressure load cases, were implemented. The original GE/EPRI functions were maintained. More significant differences occur between the two analyses for the h_2, h_3, and h_4 functions.

- The J-estimation scheme for welded pipes (LBB.ENG3) developed in Task 1 was implemented into NRCPIPE. This method incorporates both the weld and base metal stress-strain curves.

- A revised algorithm for the R6, Revision 3, Option 1 method was implemented into the NRCPIPE Code.

- The Dimensionless Plastic-Zone Parameter analysis developed in the Degraded Piping Program - Phase II was added.

2.3.2 Summary of Capabilities and Improvements to NRCPIPES

A revised version of the NRCPIPES code (Version 2.0) was developed during this reporting period. This section summarizes all the improvements made and new capabilities added to the NRCPIPES code.

User-Friendly Improvements

- The Output File includes a problem title and the Version Number of the Code. It also includes the date when the code was last modified.

- Information regarding limitations and the definition of certain terms were put on interactive screens.

- The User's Manual was updated to reflect changes to the code, provide more sample problems, and included a section on running the analysis in a batch mode.

J-Estimation Capabilities and Improvements

- The SC.TNP and SC.TKP analyses each have two options for a length parameter (L) used in these analyses. The original versions used this length parameter equal to the pipe thickness. From this project, comparisons with finite element analyses showed that this length parameter was a function of the strain hardening exponent. The original solutions with L = t are called SC.TNP1 and SC.TKP1 whereas the new solutions with L = f(n) are called SC.TNP2 and SC.TKP2.

- The SC.ENG J-estimation scheme developed in Task 2 for internal surface cracks for bending and combined bending and pressure loads was implemented into the code. The SC.ENG

method uses two algorithms to calculate equivalent thickness based on either the Net-Section-Collapse or the Kurihara Modification to Net-Section-Collapse analysis. These algorithms were implemented into the code and identified as SC.ENG1 and SC.ENG2 methods.

- The Net-Section-Collapse (limit load) solutions given as output with the SC.TNP, SC.TKP, and SC.ENG solutions is the original Net-Section-Collapse solution, but modified for long cracks to account for crack closure if the crack length extends below the neutral axis.

- The revised algorithm for the R6, Revision 3, Option 1 method developed in Task 2 was implemented into the NRCPIPES Code.

- The Dimensionless Plastic-Zone Parameter analysis developed in the Degraded Piping Program - Phase II was added.

ASME Section XI Criteria

- A capability to allow the user to calculate allowables based on ASME Section XI - Appendix C for austenitic pipes was added. Three analysis options were incorporated.

    1. Given the flaw size, the program calculates the allowable bending stress.

    2. Given the stress state and the flaw depth, the allowable flaw length is calculated.

    3. Given the stress state and the flaw length, the program calculates the flaw depth.

- A capability to allow the user to calculate allowables based on ASME Section XI - Appendix H for ferritic pipes was also added. Three analysis options were incorporated.

    1. Given the flaw size, the program calculates the allowable bending stress.

    2. Given the stress state and the flaw depth, the allowable flaw length is calculated.

    3. Given the stress state and the flaw length, the program calculates the flaw depth.

- A capability to allow the user to perform calculations based on ASME Section XI Code Case N-494-2 Deformation Plasticity Failure Assessment Diagram (DPFAD) was added.

  The DPFAD approach has two options in the code case:

  Option 1 - Determine the acceptability of pipe with a flaw for continued service
  Option 2 - Calculate allowable bending stress given a flaw size

  The failure assessment diagrams used in the Code case calculations for ferritic and austenitic piping are shown in Figures 2.1 and 2.2. The austenitic pipe curve was recently approved and should be in the 1995 Addenda as Code Case N-494-3. Curve fitting algorithms

were applied to the ASME supplied data points and the resulting equations are also shown in Figures 2.1 and 2.2. These equations have been implemented into NRCPIPES.

2.3.3 User's Manuals

The manuals for both of the codes (NRCPIPE and NRCPIPES) have been updated and modified. Several new sections have been written to provide additional guidance to the user.

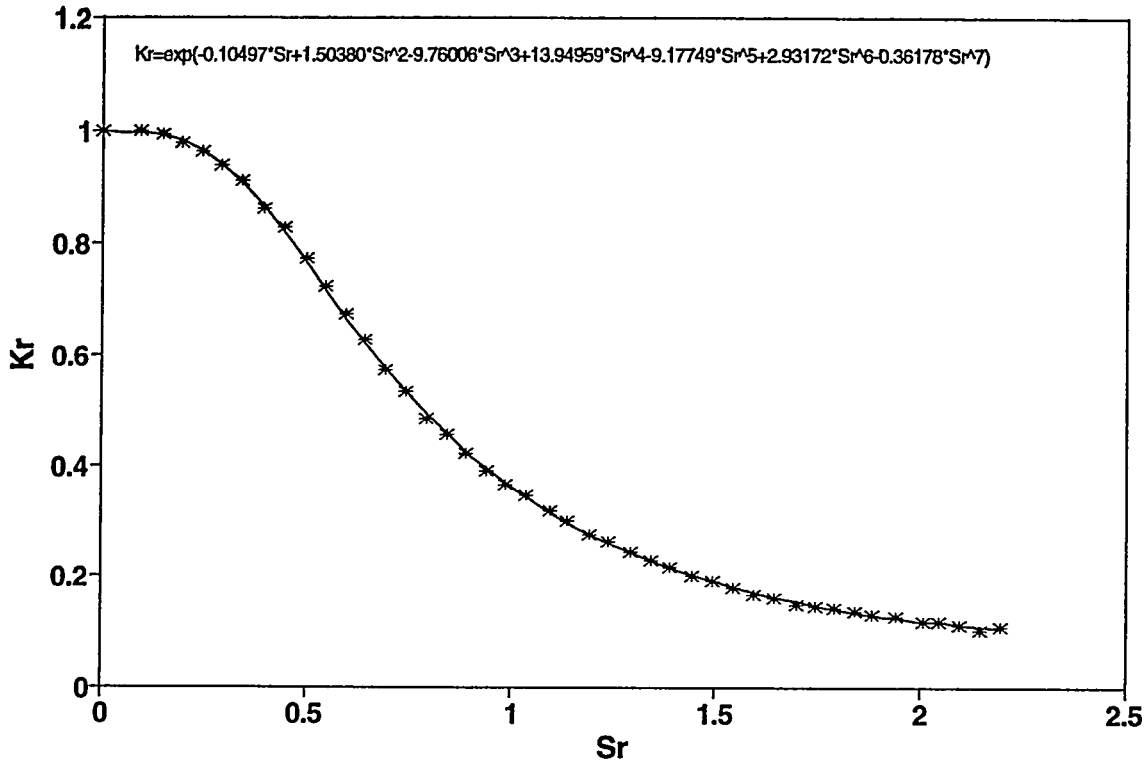

Figure 2.1 ASME Code Case N-494-2 FAD curve for ferritic pipe flaw evaluation

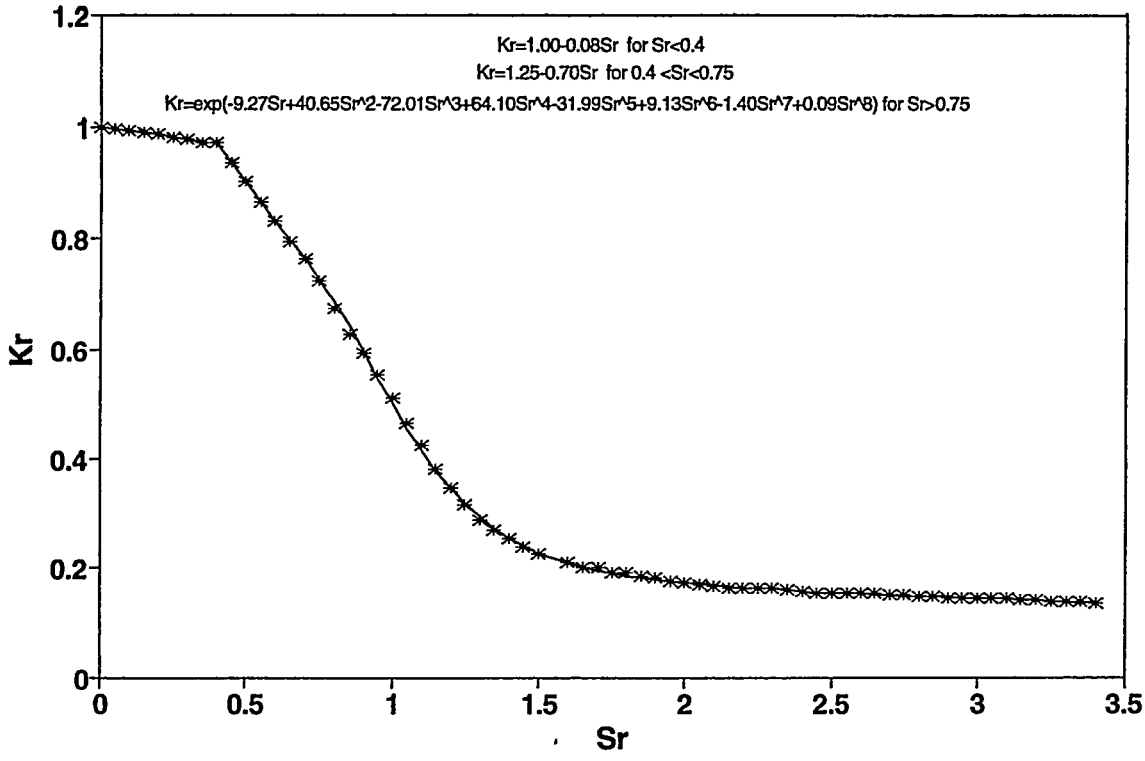

Figure 2.2 ASME Code Case N-494-3 FAD curve for austenitic pipe flaw evaluation

3. TASK 8 ADDITIONAL EFFORTS

3.1 Task Objective

The objective of this task is to conduct analyses or experiments needed to clarify issues that develop during the course of this program. To date, seven subtasks have been initiated.

3.2 Task Rationale

When the program was initiated, it was realized that the results obtained during the course of the tasks may require additional efforts to be undertaken. This task was, therefore, created. All work in this task is as a result of contract modifications to the original program.

3.3 Task Approach

The seven subtasks involving additional efforts are:

Subtask 8.1 Validity Limits on J-R Curve Determination
Subtask 8.2 Stainless Steel SAW Fusion-Line Toughness
Subtask 8.3 Update PIFRAC Data Files
Subtask 8.4 Develop Database for Circumferentially Cracked-Pipe Fracture Experiments
Subtask 8.5 Data File Conversion from HP to IBM Format
Subtask 8.6 ASME Section III Allowable Stress Limits
Subtask 8.7 Microbiologically Induced Corrosion (MIC) Pipe Experiment

Progress in Subtasks 8.3, 8.4, 8.6, and 8.7 is discussed below. The other subtasks (except Subtask 8.5) are discussed in separate topical reports.

3.4 Subtask 8.3 Update PIFRAC Data Files

3.4.1 Objective

The objective of this effort is to update the PIFRAC database (Ref. 3.1) and to include data from NRC-sponsored programs and industry-funded programs to the extent that these data are readily available.

3.4.2 Rationale

PIFRAC, a computerized database for material properties of nuclear grade piping materials, which was developed under other NRC funding, was last updated in 1989. Since that time, considerable data have been developed from NRC-sponsored programs and from a number of industry-funded programs. The NRC desires that the PIFRAC database be updated to include data from the NRC-sponsored programs and the industry-funded programs.

3.4.3 Approach

In order to obtain material data (J-R, tensile, Charpy) several programs and organizations were identified as possible sources. The required data were obtained in a variety of formats such as electronic, tables, and graphs. Using shell scripts, basic programs, etc., these data were first transferred to text files and after quality assurance plots, the data were transferred to dBASE III files.

3.4.4 Progress

The tensile test files include the entire stress-strain curve as well as yield, ultimate, percent elongation, and reduction of area values. The J-R curve specimen files include all of the data needed to recalculate the J-R curves, i.e., specimen dimensions, load, displacement, crack growth, as well as Deformation and Modified J-R curve values. The prior version of PIFRAC (Version 2.0 for PC use) included 325 tensile tests and 375 J-R specimen test files, as well as chemical analyses and Charpy data when available.

The progress for data implementation from each program or organization is described below.

Degraded Piping Program - Phase II. This was an NRC program conducted at Battelle. The previous version of PIFRAC contained most of the data developed in this program. A total of seven J-R specimens and four tensile specimens were added to the database.

IPIRG-1. A total of 76 J-R specimen files and 47 tensile specimen files were added to the PIFRAC database.

Short Cracks in Piping Welds program. A total of 66 J-R specimen files, 33 tensile specimen files, and 10 Charpy curve data files were added to the PIFRAC database.

Ontario Hydro. A total of 91 J-R specimen files and 75 tensile specimen files were added to the PIFRAC database.

General Electric. A total of 17 J-R specimen files and four tensile specimen files were added to the PIFRAC database.

Westinghouse. A total of 15 J-R specimen files were incorporated into the PIFRAC database.

Argonne. A total of 100 J-R specimen files and 304 tensile specimen files were added to the PIFRAC database.

Babcock and Wilcox. No data from Babcock & Wilcox were received, although they were requested several times.

LBB Project in Korea. Only tensile data received from Sung Kyan Kwan University (Republic of Korea) were implemented into PIFRAC. Ninety specimens were incorporated into PIFRAC. J-R curve files were not included in PIFRAC since they contained only J and Δa values. Load, displacement, crack growth, and specimen dimensions data may be available in the future.

DTRC. A total of 24 J-R specimen files out of 74 specimen tests identified from past programs were incorporated into the PIFRAC database.

IPIRG-2. A total of 54 J-R specimen files and 21 tensile specimen files were added to the PIFRAC database.

MEA. Most of the J-R and tensile data developed by MEA were already in PIFRAC. During quality assurance checks of these data we identified 73 J-R specimens that required corrections to the load-displacement data. Original raw test data (load-displacement) for each of the specimens were obtained from MEA and compared with the PIFRAC values. Additional data points were added if there were unstable crack jumps in the carbon steel specimens. (These crack jumps occur at 288 C [550 F] and are due to dynamic strain aging.) These files were translated from HP9845 disks to IBM-PC ASCII files. Overlay plots of raw data and PIFRAC data were created to identify the appropriate modifications.

Modifications (addition, deletion, or changes) were made to 72 J-R specimen files. One MEA specimen was deleted from the database. The corrected data were implemented into PIFRAC. Additionally, several data points in the tensile specimen files in the prior version of PIFRAC also needed correcting.

3.5 Subtask 8.4 Develop Database for Circumferentially Cracked-Pipe Fracture Experiments

3.5.1 Objective

The objective of this subtask is to develop a database of circumferentially cracked-pipe fracture experiments conducted throughout the world.

3.5.2 Rationale

In addition to Battelle, a number of other organizations have conducted, and are conducting, pipe fracture experiments on circumferentially cracked pipe. To date, there is no single reference, or database, that lists the test conditions and results for these experiments. Such a database would be useful to those individuals assessing the validity of analytical or Code approaches in that the appropriate experiments necessary for confirming the approaches would be readily identified. Also, such a database would be helpful in eliminating any redundancy in efforts between organizations.

3.5.3 Approach

As part of this effort, Battelle has developed a database of circumferentially cracked-pipe fracture experiments, CIRCUMCK.WK1. The format for the database is a Lotus® spreadsheet. The database, in its current form, includes the test conditions, experimental results, and applicable material property data for over 700 circumferentially cracked-pipe fracture experiments. Table 3.1 is a comprehensive list of countries and organizations for which data are included in the database. Table 3.2 is a list of the test parameters (i.e., test conditions, experimental results, and material property data) that are included in the database for each experiment.

3.5.4 Progress

Some of the data represented in Table 3.1 already existed in journals, but much of the data did not. In those cases, it was necessary to contact the researcher that conducted the experiments in order to get the data from their files. Once we received responses to the requests we sent out, we entered the data into the database. The database currently has data for over 700 pipe fracture experiments. The database is structured in four major sections on the basis of crack geometry: uncracked, through-wall-cracked, surface-cracked, and complex-cracked pipe experiments. Each of these major sections is further separated by loading conditions, i.e., four-point bending, four-point bending plus internal pipe pressure, axial membrane loading, inertial loading, and pipe system experiments. Finally, each set of data is identified by organization, program, and references.

3.6 ASME Section III Allowable Stress Limits

3.6.1 Objective

The objective of this effort was to determine the effect of changing the allowable stress value proposed in Section III of the ASME Code, on pipe flaw evaluation criteria.

3.6.2 Rationale

Two changes to the ASME Section III design stress limit rules have been proposed to increase the maximum allowable calculated stresses assuming elastic analyses. The first design rule change increases the maximum allowable stresses from $3S_m$ to $4.5S_m$ for pressure plus inertial stresses. The second design rule change increases the maximum design stresses to $7S_m$ for pressure plus secondary stresses.

In the ASME Section XI pipe flaw evaluation criteria, i.e., IWB-3640, IWB-3650, Appendix C, Appendix H, and Code Case N494-2, the stresses used in the flaw evaluation analyses are the elastic stresses from Section III of the Code. Hence, any major change to the allowable stresses in Section III can have an impact on the Section XI pipe flaw evaluation procedures. In addition, the increase of the allowable stresses will also have significant impact on the acceptance of piping LBB submittals. LBB evaluations also use stresses calculated assuming elastic analyses.

Table 3.1 List of organizations for which data are included in the circumferentially cracked-pipe fracture database, CIRCUMCK.WK1

Organization	Country
Battelle-Columbus[a]	USA
David Taylor Research Center	USA
Westinghouse	USA
MPA-Stuttgart	Germany
Institut für Reacktorbaulements	Germany
Rheinisch-Westfalischer TUV	Germany
Interatom GmbH	Germany
Seimens/KWU	Germany
Fraunhofer-Institut fur Werkstoffmechanik	Germany
ENEA	Italy
JAERI	Japan
Mitsubishi Heavy Industries	Japan
NUPEC	Japan
Hitachi	Japan
CRIEPI	Japan
EDF	France
CEA	France
Welding Institute of Canada	Canada
IVO International	Finland

(a) Nuclear as well as oil and gas industry programs.

Table 3.2 List of test parameters, results, and material property data included in CIRCUMCK.WK1 database

Test Parameters
Data Record Book Number
Experiment Number
Pipe Material Identification Number
Pipe Material
Outside Diameter
Schedule
Wall Thickness
Test Temperature
Inner Span for Four-Point Bending Experiments
Outer Span for Four-Point Bending Experiments
Test Pressure
Crack Length
Crack Depth
Experimental Results
Load at Crack Initiation
Maximum Load
Moment at Crack Initiation
Maximum Moment
Load Cycles for Cyclic Tests
Material Property Data
Yield Strength
Ultimate Strength
Percent Elongation
Reduction in Area
Ramberg-Osgood Coefficients (σ_o, ϵ_o, α, n)
J-value at Crack Initiation
dJ_D/da (initial slope of J-R curve)
Extrapolated J_D-R Curve Constants (J_i, C_1, m)[(a)]
Charpy Upper Shelf Energy (full-size specimen)
Room Temperature Charpy Energy (full-size specimen)
Room Temperature Charpy Shear Area Percent

(a) $J = J_i + C_1 (\Delta a)^m$

For the first proposed design rule change, it is relatively easy to show that the proposed design rule stress changes would significantly reduce the inherent flaw tolerance of the piping system. In the ASME Section XI pipe flaw criteria, the flow stress is the highest stress that an unflawed pipe could tolerate. The flow stress is $2.4S_m$ for ferritic pipe or $3S_m$ austenitic pipe. In examining the Section XI criteria closer, with the safety factors for Emergency and Faulted Stress Limits, the highest stress ($P_m + P_b$) that a flaw larger than the workmanship standards of Article IWB-3514 can tolerate is less than $2.2S_m$ for carbon steels and less than $2.75S_m$ for austenitic steels. Since inertial and pressure stresses are considered load-controlled or primary stresses ($P_m + P_b$), the $4.5S_m$ value is well above the limiting value for flaw sizes that just exceed the Article IWB-3514 workmanship standards. Consequently, if piping (approved by the proposed design rule changes to Section III) developed a flaw larger than that allowed by the workmanship standards, then the current rules would require that pipe be repaired or replaced. Since the proposed new stress limits are twice as high as the allowable stress levels for flaws that just exceed the workmanship standards, there may even be concern about the tolerance of pipe with allowable flaws per ASME Section XI, Article IWB-3514 with the proposed design rule change.

The big question to be addressed for this design rule change is whether inertial stresses truly act as primary or load-controlled stresses. Results from the IPIRG-1 program showed that for large flaws, where the nominal stresses were below the yield strength of the piping materials, the inertial stresses acted as primary stresses for fracture (Ref. 3.2). In fact, piping system experimental results from the IPIRG-1 program showed that if the flaw was large and the failure stresses were below yield, then even the thermal expansion and seismic anchor motion stresses acted as primary stresses for pipe fracture analyses (Ref. 3.3). It is not known how a cracked pipe subjected to inertial stresses that are above yield will behave. This evaluation would take considerably more effort than possible in this task.

It should also be noted that piping designed to the proposed stress limits would not appear to satisfy the requirements for LBB relief of pipe whip restraints or jet impingement shields as per NRC's S.R.P. 3.6.3. This is because the LBB analysis also uses stresses calculated using elastic assumptions in the elastic-plastic fracture mechanics analysis.

The effect of the second proposed stress limit of $7S_m$ (with $6S_m$ being thermal-expansion and seismic-anchor-motion-induced stresses and $1S_m$ pressure stress) on critical flaw sizes can be analyzed from a simple static analysis. The thermal expansion and seismic-anchor-motion stresses are truly displacement-controlled stresses. For these stresses, it is appropriate to make a nonlinear correction to the elastic stresses to account for yielding. This can be done as long as the primary stresses are below yield, which is the case with the pressure stresses being limited to $1S_m$.

An evaluation of the critical surface-flaw sizes with an elastic-plastic correction to the elastic secondary stresses was conducted and is described in the following section. Since stainless steels have considerably different strain-hardening behavior than ferritic nuclear pipe steels, both were evaluated. Such a nonlinear correction for displacement-controlled stresses can be developed by conducting finite element analyses of an uncracked pipe using the stress-strain curves of typical carbon and stainless steels used in nuclear piping. Once this nonlinear correction has been developed, the critical surface-flaw sizes (crack depths for given circumferential crack length) corresponding to $3S_m$, $4.5S_m$, and $7S_m$

displacement-controlled stress values can readily be determined using the Net-Section-Collapse analysis.

3.6.3 Approach

As discussed above, the allowable stress according to ASME Section III is calculated using linear elastic analysis. The currently used value of $3S_m$ is higher than the flow stress for some steels, and a value of $7S_m$ is more than twice the flow stress for most. For displacement-controlled stresses, the actual stresses and corresponding moments in the pipe do not reach these values. Consequently, a nonlinear correction can be used to compute the actual applied moment. That is, for a given rotation, the applied moment on the pipe using "realistic" elastic-plastic material properties would be less than that calculated assuming linear elastic behavior. The key assumption here is that, other than stresses due to internal pressure, all the remaining stresses above the yield stress are displacement-controlled stresses.

To assess the impact of increasing the allowable stress value from $3S_m$ to either $4.5S_m$ or $7S_m$, finite element analyses were conducted to determine the moment-rotation curve for an uncracked pipe under combined bending and pressure loads for i) linear elastic and ii) elastic-plastic behavior. The applied moments corresponding to $3S_m$, $4.5S_m$, and $7S_m$ were then determined for the two cases. Using the moment for the elastic-plastic case, the allowable flaw sizes were computed using the Net-Section-Collapse failure criterion. Comparison between the critical flaw sizes for $3S_m$, $4.5S_m$, and $7S_m$ was then made.

As discussed above, the following steps outline the analyses conducted:

- Obtain equivalent stress-strain properties using Code-allowable yield and ultimate-strength properties.
- Conduct 3D finite-element analyses for uncracked pipe. (3D brick elements were used because in the elastic-plastic regime pipe, elbow, and shell elements were found not to agree with uncracked pipe experiments [Ref. 3.4].)
- Determine moments corresponding to $3S_m$, $4.5S_m$, and $7S_m$ elastic stresses using finite element moment-rotation curves.
- Determine critical flaw sizes (a/t) and (θ/π) for the above moments using the Net-Section-Collapse criterion (Ref. 3.5) for a circumferentially surface-cracked pipe. This criterion can be stated as:

$$M = 2\sigma_f R_m^2 t(2\sin\beta - (a/t)\sin\theta) \qquad (3\text{-}1)$$

where

$$\beta = 0.5(\pi - \theta a/t) - \frac{\pi R_i^2 p}{4 R_m t \sigma_f} \quad (3\text{-}2)$$

and

M	=	failure (maximum) moment
R_i	=	pipe inside radius
R_m	=	pipe mean radius
t	=	pipe wall thickness
a	=	surface crack depth
θ	=	half-crack angle
p	=	internal pressure
σ_f	=	flow stress = $(\sigma_y + \sigma_u)/2$
σ_y	=	yield stress
σ_u	=	ultimate stress

- Develop a plot of (a/t) versus (θ/π) to define the fail and safe regions for the three values of allowable stresses ($3S_m$, $4.5S_m$, and $7S_m$) and for each material.

Specific details of the analyses are described below.

The cases used in the evaluation were:

- Pipe Size: 406 mm (16 inches), D/t = 20
- Materials: TP304 stainless steel at 288 C (550 F)
  Ferritic (A106 Grade B) steels at 288 C (550 F)
- Loading: Pressure and bending

The pipe diameter was arbitrarily selected because it is not believed to be an important parameter in these calculations.

3.6.4 Progress

3.6.4.1 Equivalent Stress-Strain Analysis

Table 3.3 shows the Code allowable material properties at 288 C (550 F) for the steels used in the analysis.

Table 3.3 ASME Code material properties

Material	PIFRAC Specimen Identification	Yield Stress (S_y), MPa (ksi)	Ultimate Stress (S_u), MPa (ksi)	S_m, MPa (ksi)
TP304	A23-1	130 (18.8)	438 (63.5)	117 (16.95)
A106 Grade B	F29-6	187 (27.1)	414 (60)	125 (18.1)

Engineering stress-strain data for the two specimens were obtained from the PIFRAC data base (Ref. 3.1). Code-allowable yield and ultimate-strength properties were used to modify the actual stress-strain curve to be consistent with Code values. Figures 3.1 and 3.2 show the actual and the Code consistent stress-strain curves for the two steels. The Code consistent stress-strain curves were used in the elastic-plastic analysis. The elastic modulus was 192 GPa (28.0 x 10^6 psi) for the A106 Grade B material and 179 GPa (26.0 x 10^6 psi) for the TP304 stainless steel pipe material.

3.6.4.2 Load Analysis

The loading on the uncracked pipe consisted of combined bending and internal pressure. As per the proposed and current ASME criteria, the internal pressure for the $4.5S_m$ and $7S_m$ cases were selected to give a longitudinal stress of S_m. For the $3S_m$ case, the pressure was selected to give a longitudinal stress of $0.5S_m$.

Linear Analysis

As described in Article NB-3652 of the ASME Boiler and Pressure Vessel Code (Ref. 3.6), the stress level is determined as:

$$7S_m = B_1 p \left[\frac{D_o}{2t}\right] + B_2 \left[\frac{D_o}{2I}\right] M \qquad (3\text{-}3)$$

For a circumferential girth butt weld crack evaluation, $B_1 = 0.5$, $B_2 = 1.0$, p = internal pressure, t = pipe wall thickness, $I = 0.0491\ (D_o^4 - D_i^4)$, D_o = outside diameter, D_i = inside diameter, and S_m = material design stress from ASME Section II, Appendix I (Ref. 3.7).

The internal pressure is obtained from

$$S_m = B_1 p \left[\frac{D_o}{2t}\right] \qquad (3\text{-}4)$$

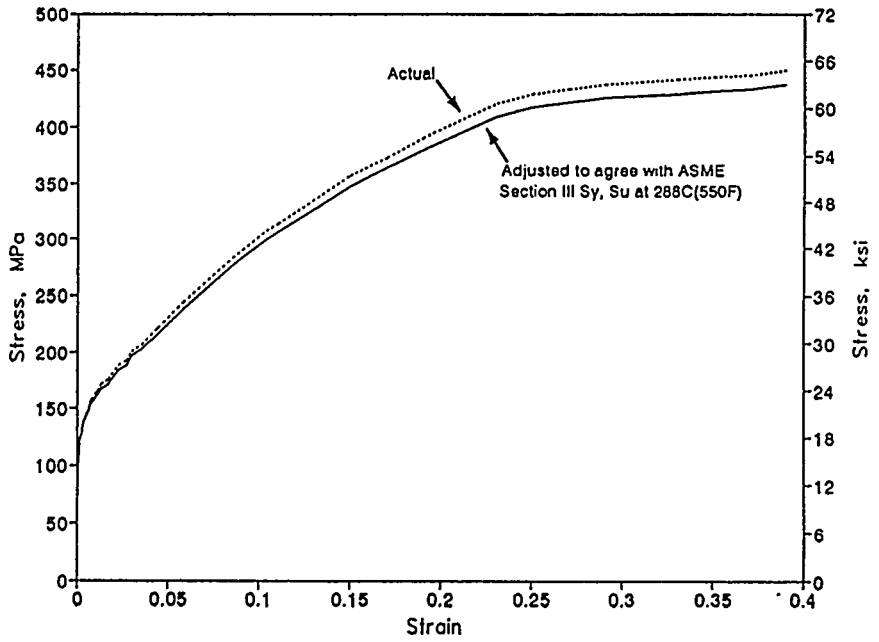

Figure 3.1 Engineering stress-strain curves at 288 C (550 F) for TP304 stainless steel for ASME Section III analysis

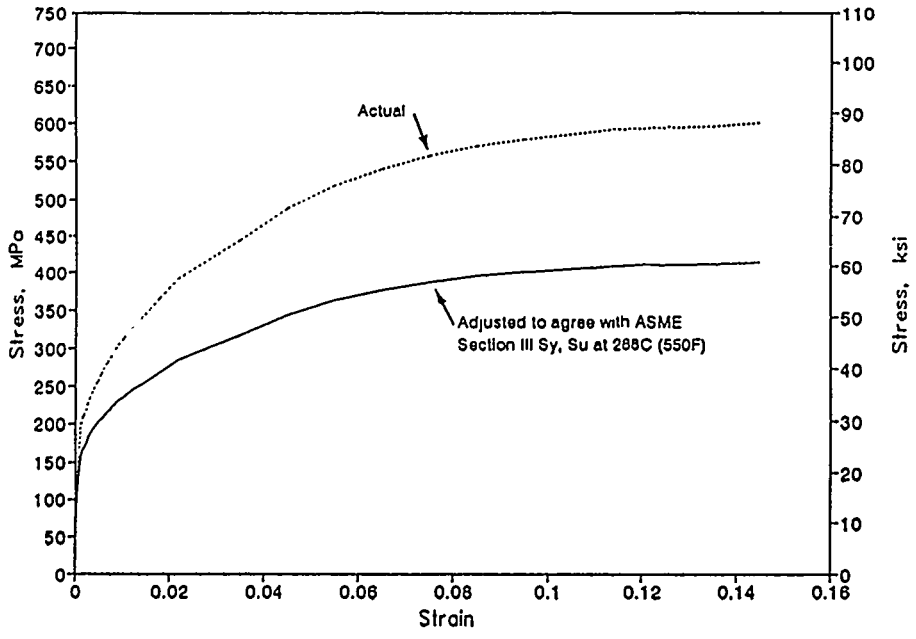

Figure 3.2 Engineering stress-strain curves at 288 C (550 F) for A106 Grade B carbon steel for ASME Section III analysis

and the moment from

$$6S_m = B_2\left[\frac{D_o}{2I}\right]M \tag{3-5}$$

The above equations also hold for the $4.5S_m$ case with $7S_m$ replaced by $4.5S_m$ in Equation 3-3 and $6S_m$ replaced by $3.5S_m$ in Equation 3-5.

Similarly, for the $3S_m$ case, the stress level is given as

$$3S_m = B_1 p\left[\frac{D_o}{2t}\right] + B_2\left[\frac{D_o}{2I}\right]M \tag{3-6}$$

the pressure is determined using

$$0.5S_m = B_1 p\left[\frac{D_o}{2t}\right] \tag{3-7}$$

and the moment from

$$2.5S_m = B_2\left[\frac{D_o}{2I}\right]M \tag{3-8}$$

The linear rotations corresponding to bending moments can easily be calculated using strength of materials. However, due to the combined pressure and bending loads, the rotations were determined from finite element analysis. Table 3.4 summarizes the internal pressure, bending moment, and rotation for the two allowable stress cases for the two different materials.

Nonlinear Analysis

A three-dimensional finite element model of an uncracked pipe using 20-noded brick elements was developed (see Figure 3.3). The model consisted of 400 elements and 2,440 nodes. A quarter section of the pipe was modeled and symmetry boundary conditions were used. In the finite element analysis, the pressure loading was applied to the inside of the pipe and an equivalent axial stress was applied at the end of the pipe as a first load step. The second load step consisted of the moment

applied as equivalent forces to the nodes on the end of the pipe. Four elastic-plastic analyses were performed, and moment-rotation results are shown in Figures 3.4 through 3.7. The $3S_m$ cases are presented in Figures 3.4 and 3.6 while the $4.5S_m$ and $7S_m$ are given in Figures 3.5 and 3.7. The moment-rotation curves for the $4.5S_m$ and $7S_m$ cases are identical since the stresses due to internal pressure are the same in both cases.

Table 3.4 Linear elastic analysis results

Material	Allowable	Internal Pressure, MPa (psi)	Bending Moment MN-m (in-lb x 10^6)	Rotation, Radians
TP304	$3S_m$	11.69 (1,695)	0.662 (5.86)	0.0258
	$4.5S_m$	23.37 (3,390)	0.921 (8.20)	0.0360
	$7S_m$	23.37 (3,390)	1.589 (14.1)	0.0619
A106 Grade B	$3S_m$	12.48 (1,810)	0.705 (6.24)	0.0255
	$4.5S_m$	24.96 (3,620)	0.990 (8.76)	0.0355
	$7S_m$	24.96 (3,620)	1.697 (15.0)	0.0613

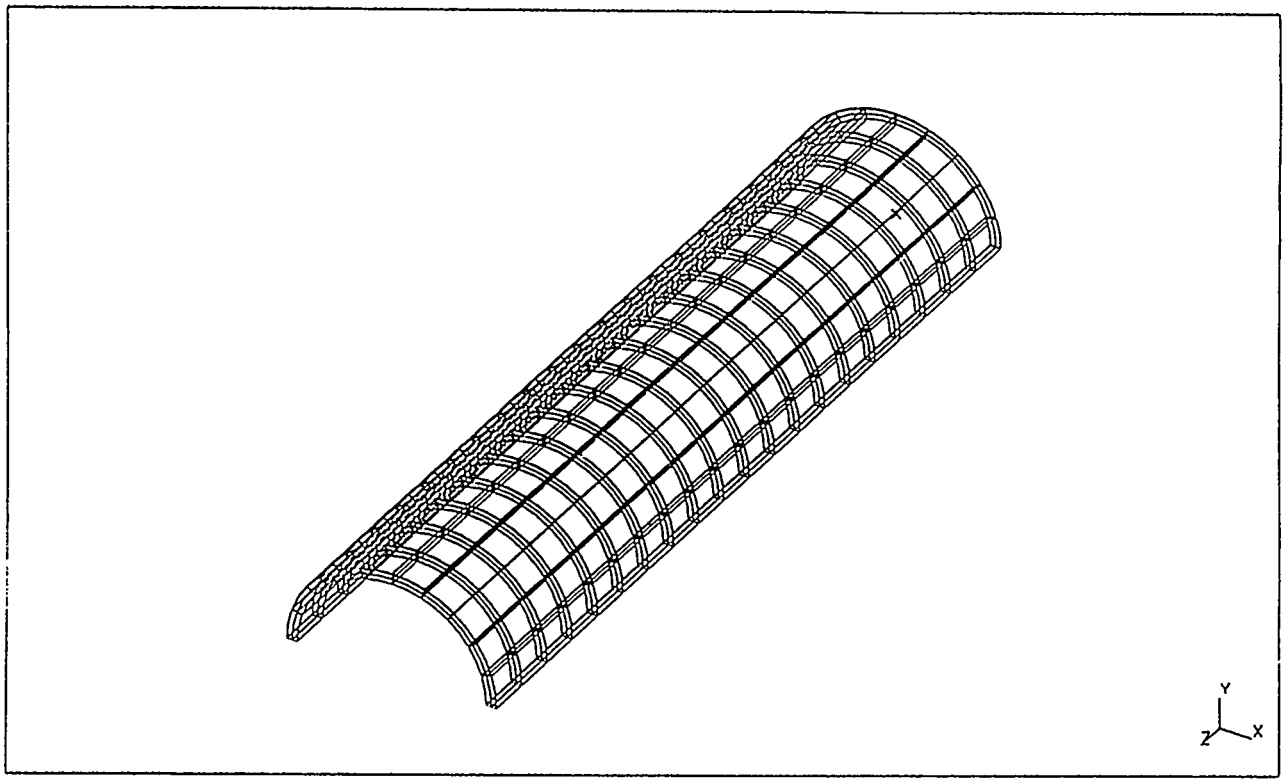

Figure 3.3 Finite element model of the uncracked pipe

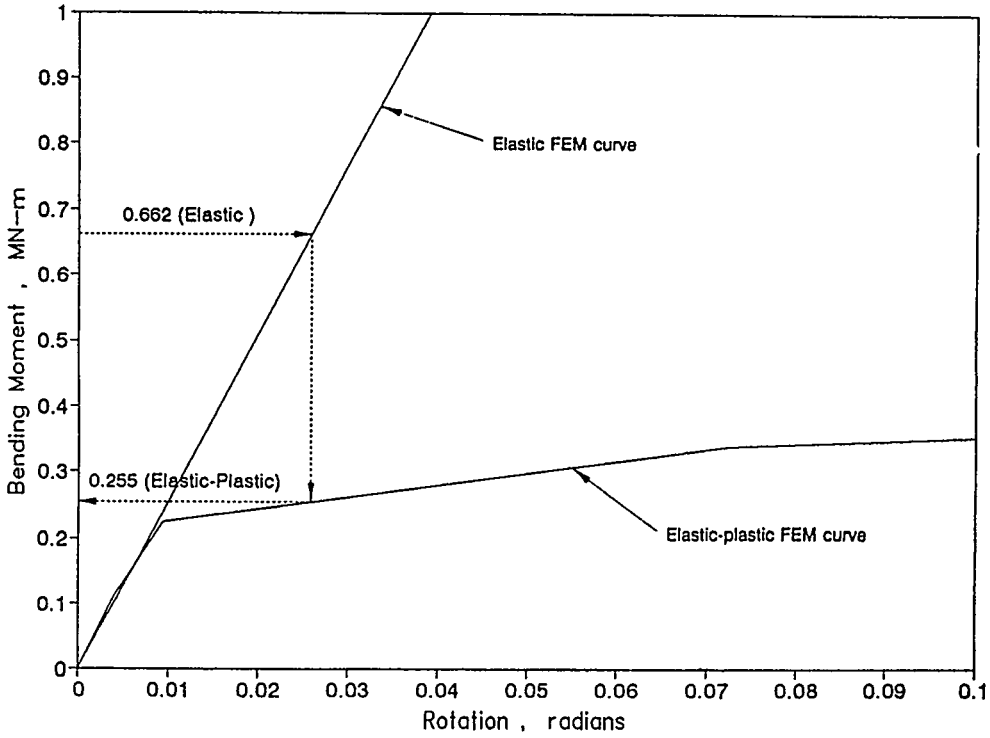

Figure 3.4 ABAQUS elastic-plastic FEM results from uncracked pipe analysis for TP304 stainless steel ($3S_m$ case)

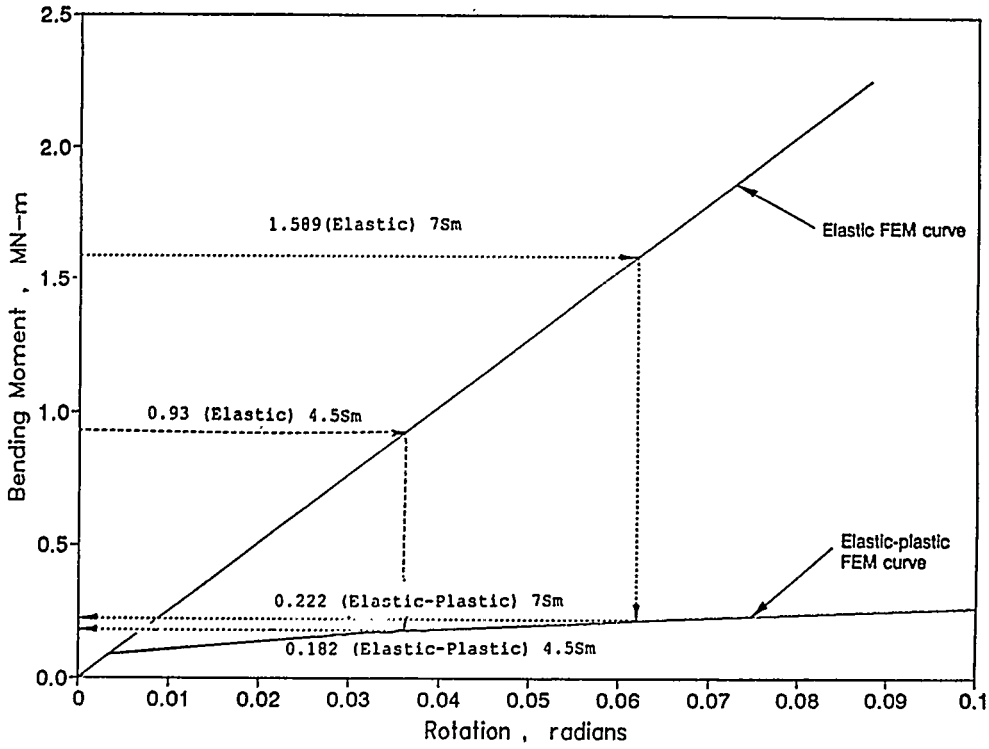

Figure 3.5 ABAQUS elastic-plastic FEM results from uncracked pipe analysis for TP304 stainless steel ($4.5S_m$ and $7S_m$ cases)

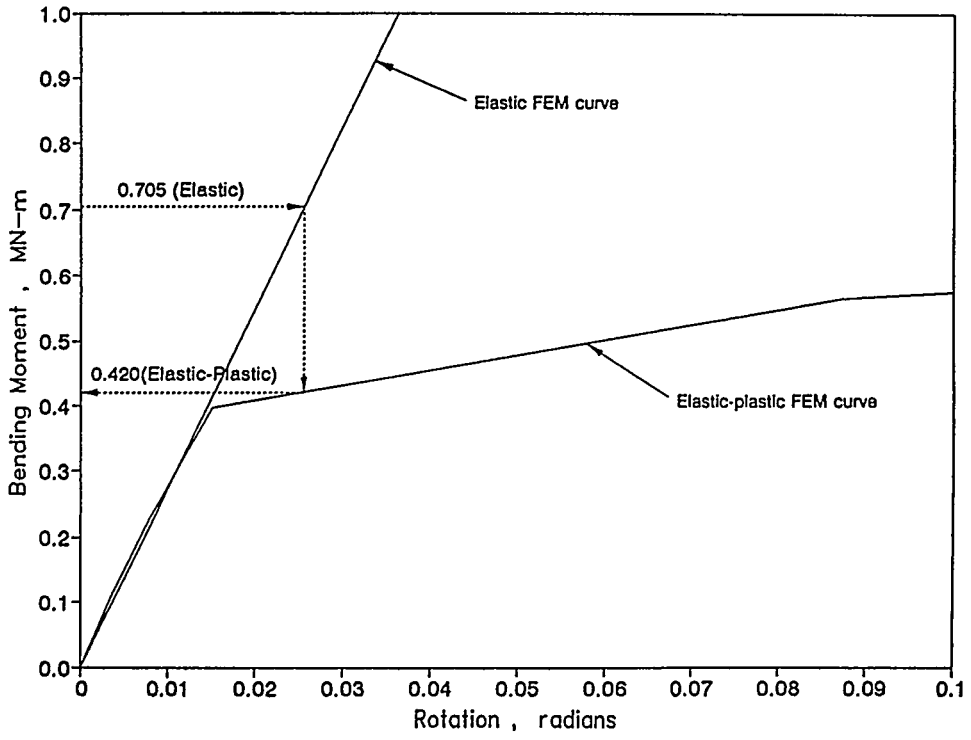

Figure 3.6 ABAQUS elastic-plastic FEM results from uncracked pipe analysis for A106 Grade B steel ($3S_m$ case)

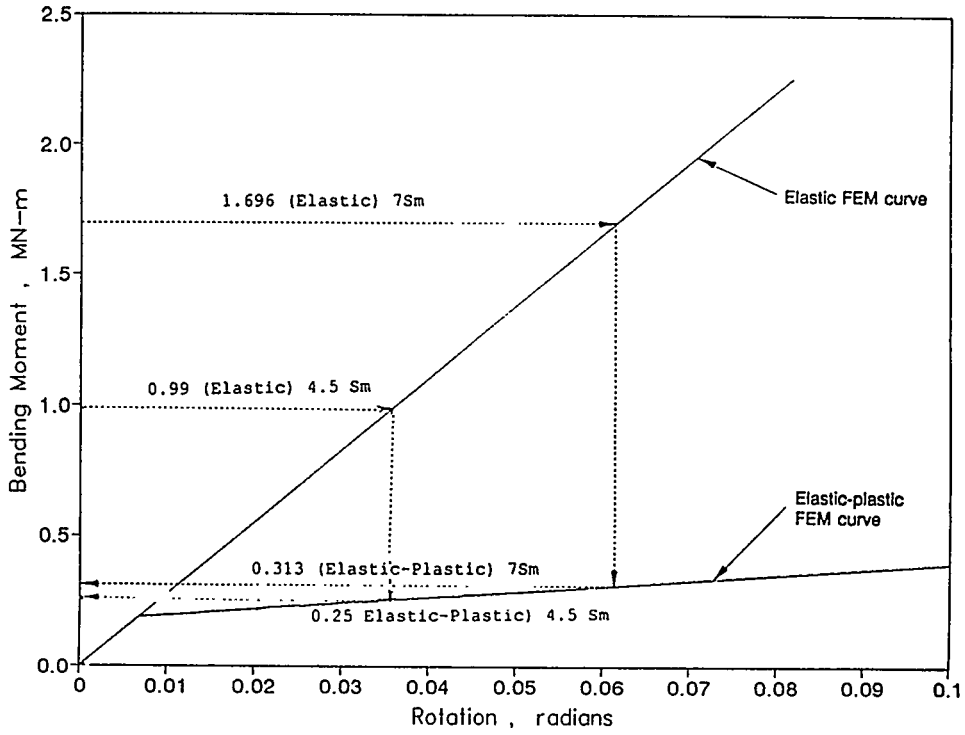

Figure 3.7 ABAQUS elastic-plastic FEM results from uncracked pipe analysis for A106 Grade B steel ($4.5S_m$ and $7S_m$ cases)

3.6.4.3 Moment Evaluation

Using the rotation calculated assumed elastic conditions presented in Table 3.4, the elastic-plastic moment at the same rotation can be determined using Figures 3.4, 3.5, 3.6, and 3.7 for the two allowable stress conditions. Table 3.5 lists the moments calculated using elastic and elastic-plastic assumptions.

Table 3.5 Allowable moments from finite element analysis

Material	Case	Elastic Moment MN-m (in-lb x 10^6)	Elastic-Plastic Moment MN-m (in-lb x 10^6)
TP304	$3S_m$	0.662 (5.86)	0.255 (2.26)
	$4.5S_m$	0.927 (8.20)	0.182 (1.61)
	$7S_m$	1.589 (14.1)	0.222 (1.96)
A106 Grade B	$3S_m$	0.705 (6.24)	0.420 (3.72)
	$4.5S_m$	0.990 (8.76)	0.250 (2.22)
	$7S_m$	1.697 (15.0)	0.313 (2.78)

3.6.4.4 Net-Section-Collapse Flaw Analysis

The last step in the analysis was to use the Net-Section-Collapse analysis (Eq. 3-1) along with moments shown in Table 3.5 to obtain a plot of a/t versus θ/π for both materials. For a given moment (M) and normalized crack length (θ/π), the normalized crack depth (a/t) was computed numerically using the bisection method. Figures 3.8 and 3.9 show the plots of a/t versus θ/π defining the fail and safe regions for the two materials. The ASME Section XI allowable planar flaw sizes (Article IWB-3514) are also shown in these figures for reference.

3.6.5 Discussion

The calculations performed in this analysis comprise a relatively simple evaluation of how a change in the ASME Section III design stresses may change the critical flaw size for pipes with Code strength values. The proposed changes to the design stress rules were to simplify the ASME Section III design rules and show that piping is much more forgiving than assumed by the current elastic stress analyses in the Code. The technical basis comes from uncracked pipe experiments. Rather than require elastic-plastic analyses, the Code Committee elected to keep the simple linear elastic analyses and, using engineering judgement and the uncracked pipe experiments as the basis, to increase the allowable stresses calculated assuming elastic conditions. Numerous simplifying assumptions were made in our evaluation that assumed that only secondary stresses were above yield. Their impact on our results are summarized below.

Using Code Minimum Strength Values

We assumed ASME Code minimum strength values at 288 C (550 F) for the pipe properties in making the nonlinear correction on the moment. Actual pipe may have higher strength values. If so, then we may have underpredicted the nonlinear moment, but the fracture analysis would be compensating because the flow stress would increase. We did not perform parametric studies to assess this tradeoff.

Net-Section-Collapse Analysis

In order to see the magnitude of the change in the flaw geometries, the Net-Section-Collapse (limit-load) analysis was used rather than an elastic-plastic analysis. This is an appropriate assumption for smaller diameter pipe and most of the stainless steel pipe (excluding cracks in stainless steel flux welds). One could use J-estimation scheme or Z-factor approaches for elastic-plastic fracture mechanics evaluations. Such corrections would lower the failure loci in Figures 3.8 and 3.9.

Displacement-Controlled Versus Load-Controlled Stresses

The key assumption inherent in this analysis was that all the stresses above the yield stress were displacement-controlled stresses. This is true for thermal expansion stresses, but not for pressure and dead-weight loads. Inertial stresses are time varying as are seismic anchor motion stresses. Inertial stresses are frequently considered primary or load-controlled, whereas seismic anchor motion stresses may be considered secondary or displacement-controlled stresses. Hence, if the inertial stresses are

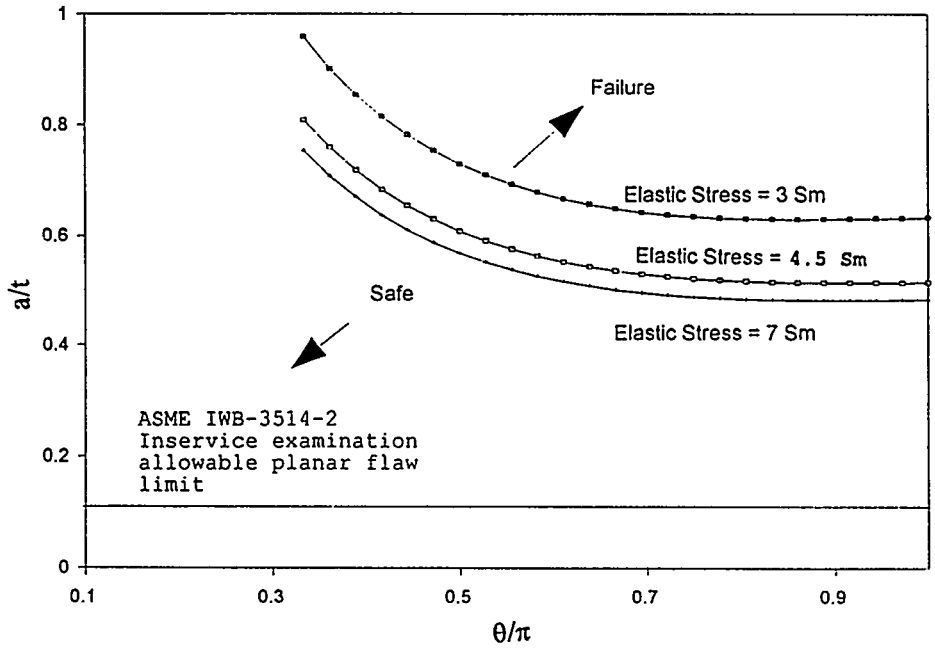

Figure 3.8 Net-Section-Collapse analysis calculated surface crack loci for pipes with $3S_m$, $4.5S_m$, and $7S_m$ displacement-controlled elastic stresses (material TP304)

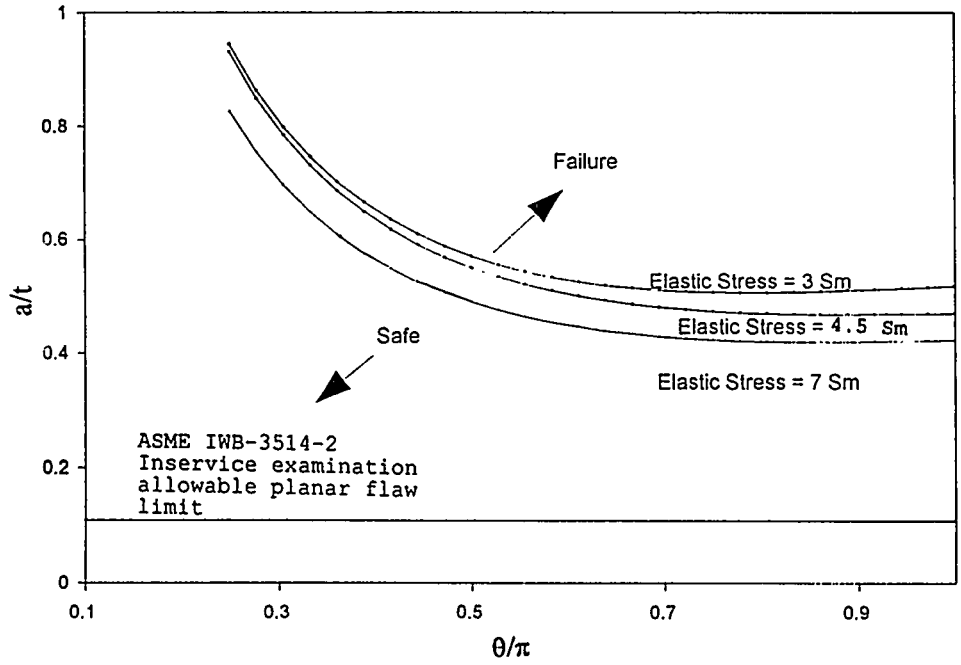

Figure 3.9 Net-Section-Collapse analysis calculated surface crack loci for pipes with $3S_m$, $4.5S_m$, and $7S_m$ displacement-controlled elastic stresses (material A106 Grade B)

above yield (as in the $4.5S_m$ proposed rule change) this analysis is not valid and in a load-controlled static analysis, failure would be predicted for pipe even with flaws acceptable by ASME Section XI, Article IWB-3514. A validated elastic-plastic dynamic cracked-pipe analysis would be needed for assessing flaw evaluation when the inertial stresses are above yield.

Quasi-Static Versus Time-History Calculations

All of these calculations were done assuming a quasi-static loading, i.e., the $3S_m$, $4.5S_m$, or $7S_m$ elastic displacement-controlled stresses were maintained for a long time. Actual dynamic loading is much more complicated, especially for real pipe systems. Flaw evaluation of inertial stresses above yield requires nonlinear time-history analysis. Plasticity, due to the crack, may also reduce the peak dynamic loads that can be applied at a cracked section. Accounting for the crack plasticity effects may raise the failure loci. On the other hand, cyclic loads associated with seismic loading have been shown to reduce the toughness of all types of steels tested to date.

3.6.6 Conclusions

The conclusions from this study on both proposed Code changes ($4.5S_m$ for inertial and pressure and $7S_m$ for secondary and pressure stresses) are given below.

- If the inertial and pressure stress limits are raised to the proposed values of $4.5S_m$, then the flaw evaluation analysis in ASME Section XI shows that any pipes with flaws greater than those allowed by the workmanship standards (in Article IWB-3514) will have to be repaired or replaced. This is because the ASME Section XI pipe flaw evaluation criteria use elastic stresses in the flaw evaluation procedures. In fact, the $4.5S_m$ stress is twice as high as the allowable Service Level C stresses at the workmanship standard flaw limits in the flaw evaluation criteria. Consequently, there may even be concern about pipe with workmanship-allowable flaws being acceptable at these high stress levels. Note that in the EPRI Piping Reliability program, the experiments were conducted on unflawed piping, and no experiments had flaws allowed by the workmanship standards in Section XI. Hence, there is no technical support for the $4.5S_m$ rule change from this viewpoint.

- The above limitation, relative to ASME flaw evaluation procedures, is very severe and may ultimately not allow piping systems with such high stresses to be approved for LBB. Again, this is because LBB in S.R.P. 3.6.3 uses elastic stresses.

- One way that the $4.5S_m$ stress limit could be justified is if the actual inertial stresses (or moments) have some nonlinear correction that is verified for pipe flaw evaluation. No data exist for flawed pipe loaded with inertial stresses at these high stress levels. The IPIRG-1 program data (Refs. 3.2 and 3.3) had experiments with large flaws, and it was shown that inertial, thermal expansion, and seismic anchor motion stresses all contributed as load-controlled stresses when the nominal stresses were below yield.

- Assuming the higher stresses are displacement-controlled (i.e., thermal expansion and seismic anchor motion), then a nonlinear correction to the elastic stresses is justified. This study showed that the effect of changing the allowable stress value in the ASME Section III Code from $3S_m$ to either $4.5S_m$ or $7S_m$ for circumferentially surface-cracked pipe lowers the failure loci as shown in Figures 3.8 and 3.9. The change in the failure loci was not large.

- For the displacement-controlled analysis, the failure loci for the two types of materials used in the analyses show that the overall shift for ferritic steels is less than that for stainless steels, even though limit-load failure is assumed for both materials. This shift is due to the strain-hardening characteristics of the two materials.

- For the displacement-controlled analysis, increasing the allowable stresses calculated using elastic assumptions to $4.5S_m$ or $7S_m$ changed the inherent flaw sizes that the piping can tolerate if the primary stresses are below the yield stress. These are still relatively large flaw sizes for both materials and are well above the Standards for Preservice Inspection Allowable planar flaws.

- This analysis suggests that changes to the ASME Section XI flaw evaluation procedures may be required in the future to account for stresses calculated assuming elastic conditions above the current $3S_m$ or $2S_y$ limits. The procedures evaluated in this effort consider the primary stress being below yield with secondary stresses above yield. For inertial stresses above yield, any change to the flaw evaluation standards would require considerable data and developments that do not currently exist.

3.7 Subtask 8.7 Microbiologically Induced Corrosion (MIC) Pipe Experiment

3.7.1 Objective

The objective of this effort was to conduct a pipe experiment on a section of 6-inch nominal diameter pipe donated by Northeast Utilities. The pipe was removed from the service water system of the Haddam Neck (Connecticut Yankee) Plant due to degradation caused by microbiologically induced corrosion (MIC) at a girth weld crack.

3.7.2 Rationale

The rationale for conducting this pipe experiment was twofold. For one, it allowed an assessment of the significance of an actual girth-weld defect, possibly enhanced by microbiologically induced corrosion, on the integrity of piping. Second, the data from this experiment provided a "real-world" assessment of the analysis methodologies developed to date for the assessment of degraded piping. The pipe fracture data developed in the past have been developed using well controlled test conditions. The flaws generally have been machined flaws, which were relatively uniform in depth. Some of the machined flaws were fatigue precracked to provide a sharp crack. The pipe wall

thicknesses also tended to be fairly uniform. In this pipe, the wall thickness was non-uniform due to the MIC. In addition, there was a circumferential flaw at the girth weld attaching the straight pipe section to an existing weld neck flange. The depth of this flaw was highly variable, ranging from 7.0 to 63.5 percent of the wall thickness, based on ultrasonic inspections carried out by inspectors at Northeast Utilities. In addition, there appeared to be a branch connection protruding from the side of this straight pipe section, which could act as a stress concentrator when the pipe section was loaded. All of these factors, i.e., the non-uniform wall thickness, the irregular flaw size, and the potential stress concentrator, complicated the analysis of this experiment. However, these are the types of complicating factors that a plant engineer must face. Consequently, data from this experiment provide insight into the uncertainties in the pipe fracture analyses that may occur due to practical considerations.

An interesting additional aspect related to this experiment is that a similar cracked weld was removed from service after being analyzed using the ASME Section XI Appendix H ferritic pipe criteria. The results of the analysis indicated that the flaw was unacceptable if the EPFM Z-factor approach was used. However, the analysis showed that the flaw was acceptable for continued service if the LEFM analysis (using a lower toughness value than used in the EPFM analysis) was used. Hence, there may be some fundamental problems with the current ASME Section XI Appendix H and IWB-3650 analysis procedures.

3.7.3 Approach

The pipe section from the Haddam Neck (Connecticut Yankee) Plant service water piping system was a 6-inch nominal diameter, Schedule 40, A53 Grade A carbon steel pipe that was 240-mm (9.5-inches) long. It was welded to a 150-pound class weld neck flange. The flaw was in the pipe-to-flange girth weld. In addition, a long-radius elbow was welded to the other end of the pipe section. Figure 3.10 is a schematic showing this section of pipe welded to the weld neck flange on one end and the long-radius elbow on the other end. Figure 3.11 is a photograph of this flange-pipe-elbow configuration. Also shown in Figure 3.11 is a closeup photograph of the inside of the pipe-to-flange weld region showing the MIC-damaged inside pipe surface.

Subthickness Charpy and 0.5T planform size compact (tension) specimens were machined from the pipe base metal material and the pipe-to-elbow girth-weld for fracture toughness evaluations. Subsized tensile specimens, with a 3.33-mm (0.131-inch) diameter gage section, were also machined from the base metal of the pipe section. Due to the small size of the weld, it was not possible to machine tensile specimens in which the gage section was totally weld metal. Consequently, no weld metal tensile data are available.

Prior to the experiment, the welds were ultrasonically and radiographically inspected to determine the pipe wall thickness and crack depth using a nuclear-certified inspector from Northeast Utilities. Once the inspections were completed, the pipe was sent back to Battelle where moment arms were welded onto the test specimen in preparation for testing. The pipe specimen was loaded under combined constant internal pipe pressure and four-point bending using the small-capacity four-point-bend frame. Figure 3.12 is a schematic of that facility. The test specimen was filled with water and pressurized to 0.7 MPa (100 psi), the operating pressure of this piping system.

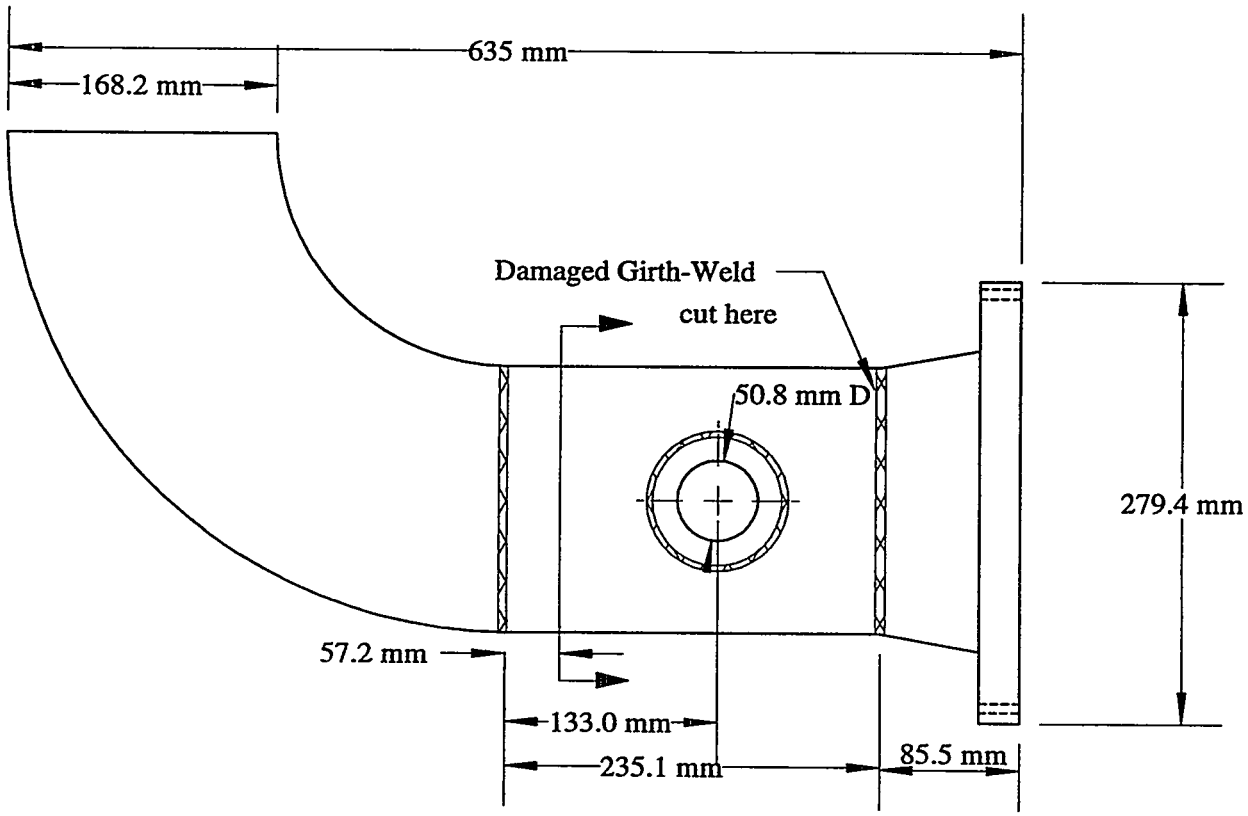

Figure 3.10 Schematic of pipe section removed from the Service Water Piping System of the Haddam Neck (Connecticut Yankee) Plant

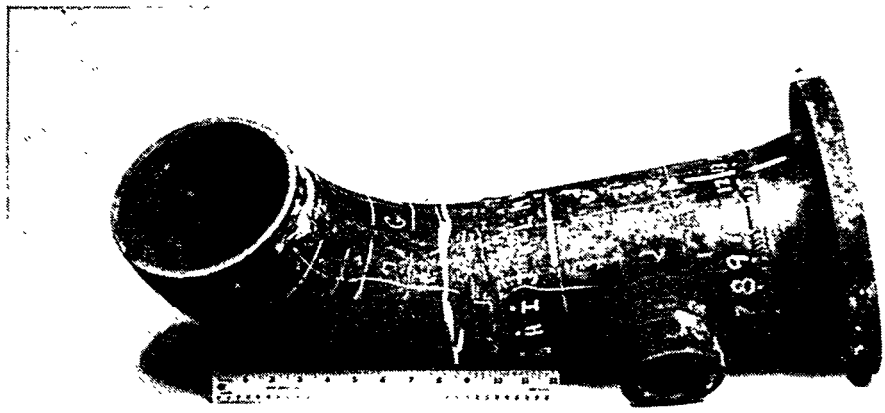

(a) Overview

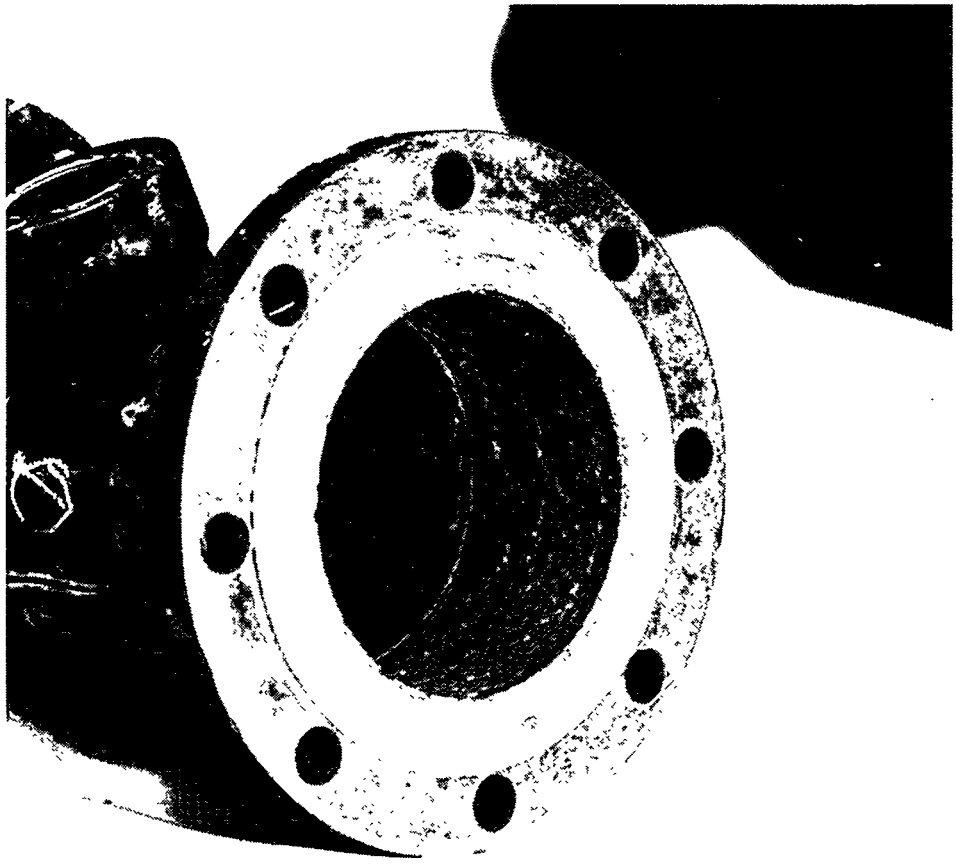

(b) Looking into flange

Figure 3.11 Photograph of the pipe section removed from the Service Water Piping System of the Haddam Neck (Connecticut Yankee) Plant

The test specimen was instrumented with inclinometers to measure crack section rotations, electric potential probes to ascertain crack initiation and crack growth, clip gages to measure crack-mouth-opening displacements, LVDTs to measure actuator displacements, and load cells in the load train to measure the applied loads.

The data were acquired on a personal computer using Labtech Notebook® data acquisition and control software. Data reduction and reporting were consistent with what was done for other experiments conducted as part of this program.

3.7.4 Results

3.7.4.1 Results from the Pretest Inspections

Prior to the conduct of the experiment the test specimen was inspected by personnel at Northeast Utilities. They measured the wall thickness of the pipe in the vicinity of the pipe-to-flange girth weld, to quantify the extent of the microbiologically induced corrosion, and measured the depth of the crack in this weld at approximately 20 locations around the pipe circumference using ultrasonic testing (UT). The results of their inspections are shown in Table 3.6 and Figure 3.13. (Table 3.6 also contains the crack depths measured optically from the post-test fracture surface.) As can be seen in Table 3.6 and Figure 3.13, the crack in the weld extended all the way around the pipe circumference and was approximately 63.5 percent of the pipe wall thickness in depth at its deepest location. The wall thickness of this nominal 7.11-mm (0.280-inch)-thick pipe had been reduced by the MIC and general corrosion such that the actual wall thickness ranged from 5.08 mm (0.200 inch) at its thinnest location to 6.48 mm (0.255 inch) at its thickest location.

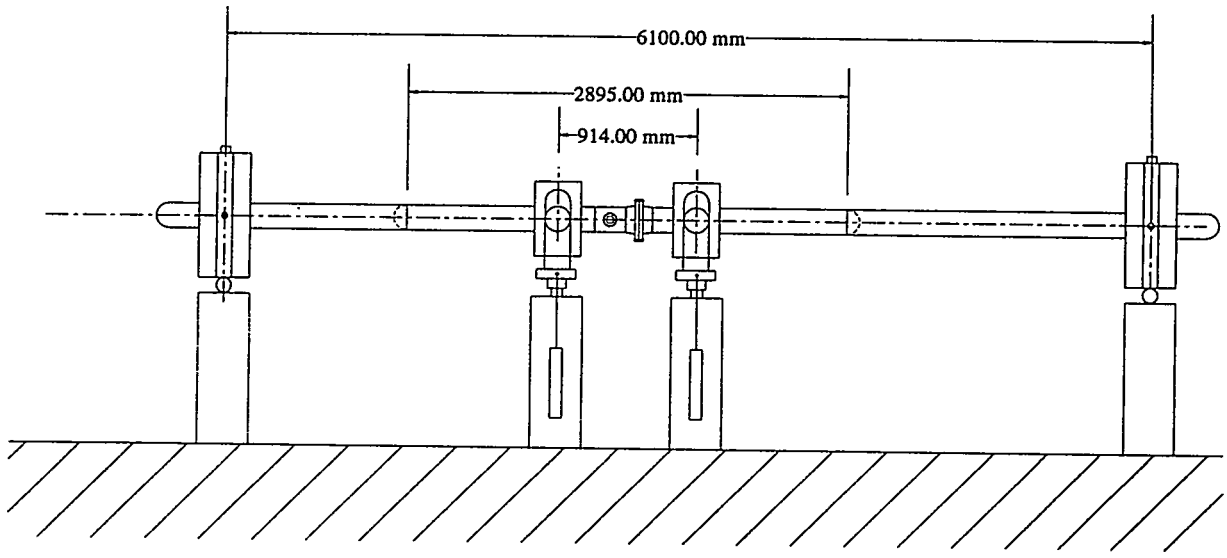

Figure 3.12 Schematic of load frame used for the Haddam Neck (Connecticut Yankee) MIC experiment

Table 3.6 Results of pretest ultrasonic inspections of the test girth weld for the Haddam Neck MIC experiment

	UT Results						Fracture Surface[a]		
Marker	tp, mm	wl, mm	pl, mm	ap, mm	ID pipe, mm	OD + Weld Crown, mm	tfw, mm	af, mm	ap, mm
1.00	6.0	7.4	5.1	0.9	156.8	173.5			
2.00	5.8	5.8	4.3	1.6	157.1	171.9			
3.00	5.6	5.1	4.2	1.4	157.6	170.4			
4.00	5.6	5.8	4.6	1.0	157.6	171.1			
5.00	6.0	6.8	5.3	0.7	156.8	171.9			
6.00	6.4	7.4	5.4	1.0	156.1	172.7			
7.00	5.8	4.9	2.5	3.4	157.1	173.5			
8.00	6.4	5.2	3.6	2.7	156.1	171.9	8.2	3.6	3.3
9.00	6.3	5.7	4.2	2.1	156.2	171.9	8.5	3.5	2.8
10.00	6.0	6.5	4.9	1.1	156.8	171.9	8.3	2.6	1.9
11.00	6.5	7.7	5.7	0.8	155.8	172.7	8.5	2.0	2.0
12.00	6.5	4.3	2.4	4.1	155.8	172.7	7.8	2.9	3.6
13.00	6.2	4.3	2.7	3.5	156.4	171.9	8.1	3.1	2.7
14.00	6.4	5.5	4.3	2.0	156.1	171.1	6.9	2.9	3.6
15.00	6.1	6.9	5.7	0.4	156.6	171.1	8.2	2.9	2.0
16.00	6.1	6.5	5.0	1.1	156.6	171.9	8.5	2.9	2.1
17.00	6.2	7.5	5.2	1.0	156.4	173.5	9.8	2.3	1.1
18.00	5.1	5.1	3.5	1.6	158.6	171.9	8.3	2.6	1.0
19.00	6.0	5.6	4.1	1.9	156.8	171.9	8.8	3.5	2.2
20.00	5.9	5.2	4.0	1.9	156.9	171.1			
21.00	5.7	5.9	4.7	1.0	157.4	171.1			

(a) No optical measurements were made between Marker Number 20 and Marker Number 7 since the pipe did not break along the initial girth weld crack in these regions when the fracture surface was broken open after the experiment. Also note that betwen Marker Number 8 and 19 the crack and pipe geometry were measured on 6.35 mm (0.25 inch) increments instead of only at the 25.4 mm (1 inch) increments used in the UT inspections. The additional optically measured values are not shown in this table.

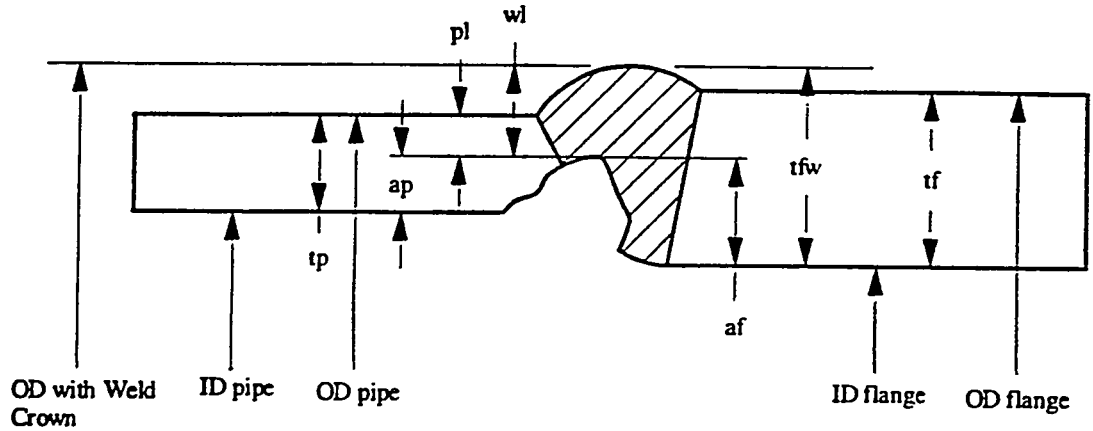

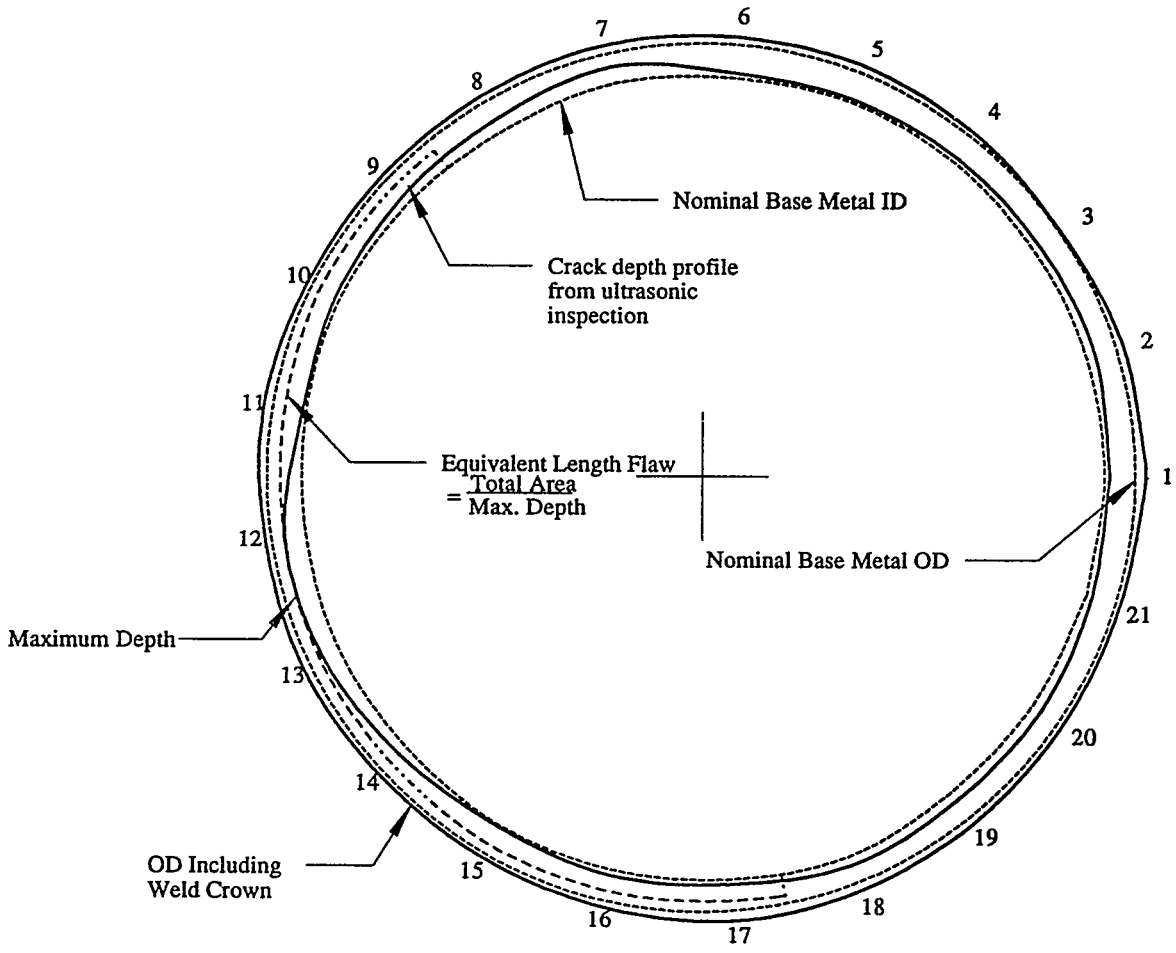

Figure 3.13 Crack profile based on Northeast Utilities ultrasonic inspections

3.7.4.2 Results from the Material Characterization Tests

Subsized tensile specimens with a 3.33-mm (0.131-inch) diameter gage section were machined from the base metal of the pipe section. Table 3.7 and Figure 3.14 show the results of the tensile tests using these specimens. Included in Table 3.7 are the yield and ultimate strength values, fracture elongation, and Ramberg-Osgood coefficients.

Compact (tension) fracture toughness specimens of the 0.5T-planform size were machined from the pipe base metal material and the pipe-to-elbow girth weld. The specimens were machined in the L-C orientation, simulating the growth of a circumferential through-wall crack. For the weld metal specimens, the notch was centered in the weld. Due to the curvature of the pipe, the thickness of the C(T) specimens was approximately 3.9 mm (0.154 inch). Table 3.8 and Figure 3.15 show the results of these fracture toughness tests for these specimens.

Table 3.7 Summary of tensile properties at 20 C (68 F) for the base metal specimens for the 6-inch nominal diameter Service Water Piping System from the Haddam Neck (Connecticut Yankee) Plant

Specimen Identification Number	Strain Rate, s^{-1}	0.2-Percent Offset Yield Strength, MPa	ksi	Ultimate Tensile Strength, MPa	ksi	Elongation[a], Percent	σ_o, MPa	ϵ_o	α	n
F54-t1	4×10^{-4}	308.6	44.8	462.6	67.1	30	308.6	0.001492	4.795	6.545
F54-t2	4×10^{-4}	298.2	43.2	450.0	65.3	31	298.2	0.001442	6.018	6.287
Average	4×10^{-4}	303.4	44.0	456.3	66.2	30.5	303.4	0.001467	6.4065	6.416

(a) Final elongations measured from total specimen length.

Table 3.8 Summary of fracture toughness values at 20 C (68 F) for the MIC base metal and weld metal specimens

Specimen Identification	J at Initiation, kJ/m^2	in-lb/in^2	dJ_D/da,[a] MJ/m^3	in-lb/in^3
		Base Metal		
DP2-F54-1	191.1	1,091	106.4	15,430
DP2-F54-2	179.2	1,023	141.4	20,510
Average	185.1	1,057	123.9	17,970
		Weld Metal		
DP2-F54W-1	84.9	485	119.8	17,370
DP2-F54W-2	82.3	470	100.4	14,560
Average	83.6	477	110.1	15,960

(a) From initial part of J-R curve between 0.152-mm (0.006-inch) and 1.524-mm (0.060-inch) of crack extension.

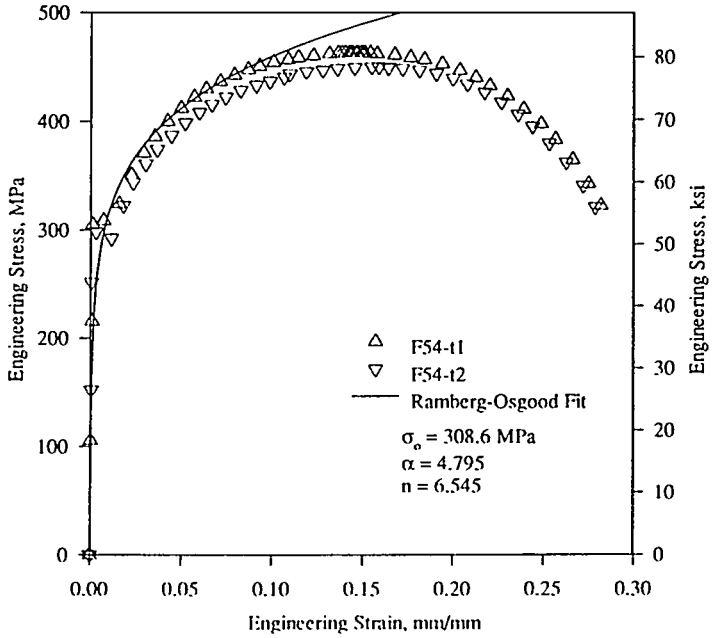

Figure 3.14 Engineering stress-strain curve for the base metal at 20 C (68 F) from the 6-inch nominal diameter Service Water Piping System removed from the Haddam Neck (Connecticut Yankee) Plant

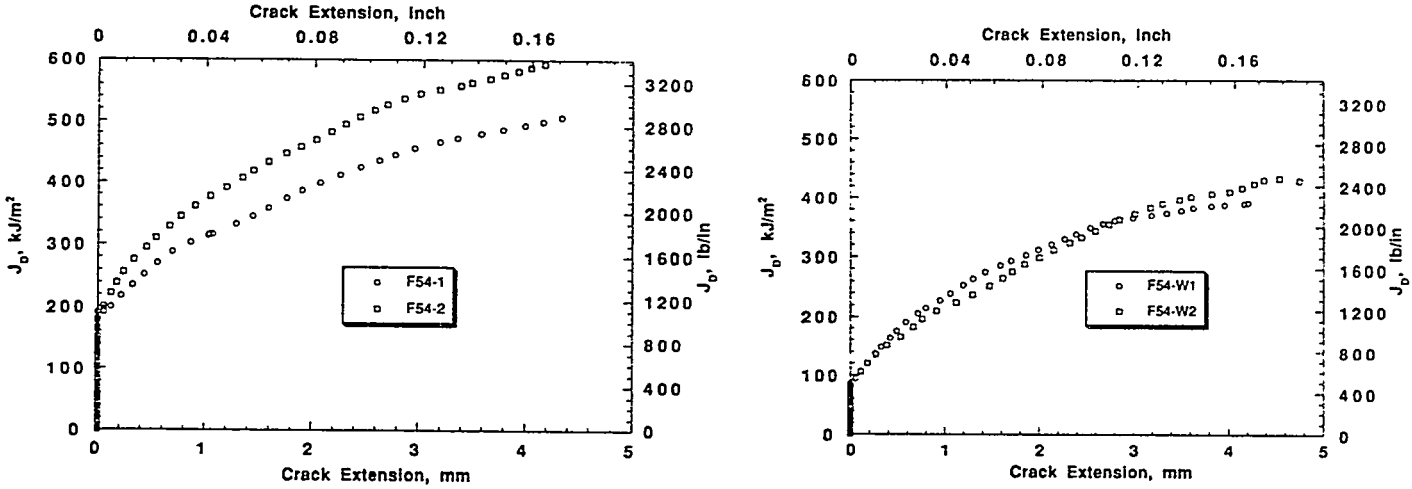

(a) Base metal (b) Weld metal

Figure 3.15 J-R curves for the base metal and weld metal at 20 C (68 F) from the 6-inch nominal diameter Service Water Piping System pipe removed from the Haddam Neck (Connecticut Yankee) Plant

Subthickness Charpy specimens were machined from the pipe base metal material and the pipe-to-elbow girth weld. The specimens were machined in the L-C orientation. For the weld metal specimens, the notch was centered in the weld. The results from the Charpy tests, energy and shear area versus temperature, are shown in Table 3.9 and Figure 3.16.

3.7.4.3 Results from the Pipe Experiment

The cracked-pipe specimen was loaded in four-point bending in the Battelle small-capacity four-point bend test frame. Figure 3.17 is a pre-test photograph of the test specimen setup in the test frame. The inner and outer spans for this test frame are 0.914 m (36 inches) and 6.096 m (240 inches), respectively. The test specimen was aligned in the load frame such that the deepest part of the crack would be in the region of maximum bending stress from the applied bending loads. The loading rate for the experiment was 1.8 mm/minute (0.07 inches/minute). In addition to the bending loads, the internal pipe pressure was maintained at a constant value of 0.7 MPa (100 psi). The test temperature was ambient, i.e., 16 C (60 F).

Table 3.10 presents the key results for this experiment. Included in Table 3.10 are the pipe and crack dimensions, pertinent material property data (i.e., base metal yield and ultimate strengths and J_i value for the weld metal), the load and moment at crack initiation, and the maximum load and maximum moment for the experiment.

Figure 3.18 shows the total applied load versus ram displacement relationship for this experiment. The maximum total applied load for this experiment was 46.6 kN (10,476 pounds).

Figure 3.19 shows the crack section moment data as a function of the rotation data for this experiment. The rotation data shown in Figure 3.19 are the half rotation angle (ϕ), i.e., the angle from one end of the deflected pipe to its original horizontal position, see Figure 3.19. The maximum applied moment for this experiment was 60.37 kN-m (534.3 in-kips).

Figure 3.20 is a plot of the crack centerline[(a)] direct-current electric potential (d-c EP) versus crack centerline crack-mouth-opening displacement (CMOD). Also included on this figure are the total applied load data. From the d-c EP versus CMOD data one can determine crack initiation. Crack initiation is defined as the point on the d-c EP versus CMOD data plot where the slope increases. From Figure 3.20, it can be seen that the slope of the d-c EP versus CMOD plot increases at a CMOD value of approximately 2.77 mm (0.11 inches). From Figure 3.20, the applied load at this CMOD values is approximately 45.72 kN (10,280 pounds). This is 98 percent of the maximum load for this experiment.

Figures 3.21, 3.22, and 3.23 show metallographic sections through the pipe-to-flange girth weld between Markers 12 and 13, 16 and 17, and 3 and 4, respectively. In all photographs, the flange material is to the left of the weld and the pipe material is to the right of the weld. The scale shown is

(a) Since the crack in this specimen extended completely around the pipe circumference there is really no crack centerline. In this context the crack centerline is the location along the crack front where the crack is the deepest, and due to the setup of the experiment, the region of highest bending stress.

Table 3.9 Base metal and weld metal Charpy impact data (1/4-thickness specimens)

Specimen	Temperature, C	(F)	Energy, J	(ft-lbs)	Shear Area, Percent
		Base Metal			
B-1	23	(73)	22	(16)	100
B-2	23	(73)	22	(16.5)	100
B-3	288	(550)	21	(15.5)	100
B-4	-23	(-9)	25	(18)	95
B-5	-76	(-105)	2.0	(1.5)	0
B-6	0	(32)	24	(17.5)	100
B-7	-45	(-49)	16	(12)	55
B-8	-45	(-49)	2.7	(2.0)	10
B-9	-34	(-29)	19	(14)	95
B-10	-32	(-26)	22	(16)	90
B-11	-58	(-72)	2.7	(2.0)	0
		Weld Metal			
W-1	23	(73)	15.6	(11.5)	100
W-2	23	(73)	15.6	(11.5)	100
W-3	288	(550)	15	(11)	100
W-4	-76	(-105)	14	(10)	100
W-5	-76	(-105)	12	(9)	95
W-6	-238	(-396)	1.4	(1)	0
W-7	-238	(-396)	1.4	(1)	0
W-8	-108	(-162)	2.0	(1.5)	0
W-9	-86	(-123)	8.8	(6.5)	65

Table 3.10 Key results for the Haddam Neck (Connecticut Yankee) MIC pipe experiment

Pipe Diameter, mm	Wall Thickness, mm	a/t	2c/πD	Base Metal Yield Strength, MPa (ksi)	Base Metal Ultimate Strength, MPa (ksi)	Weld Metal J_i Value, kJ/m^2 (in-lb/in^2)	Moment at Crack Initiation, kN-m (in-lbx10^3)	Maximum Moment, kN-m (in-lbx10^3)
168.7[a]	6.02[b]	0.60[c]	1.0	301 (44.0)	456.3 (66.2)	83.6 (477)	59.28 (524.7)	60.37 (534.3)

(a) Excluding weld crown.
(b) Average value and excluding weld crown.
(c) Maximum crack depth divided by pipe wall thickness at the location of the maximum crack depth.

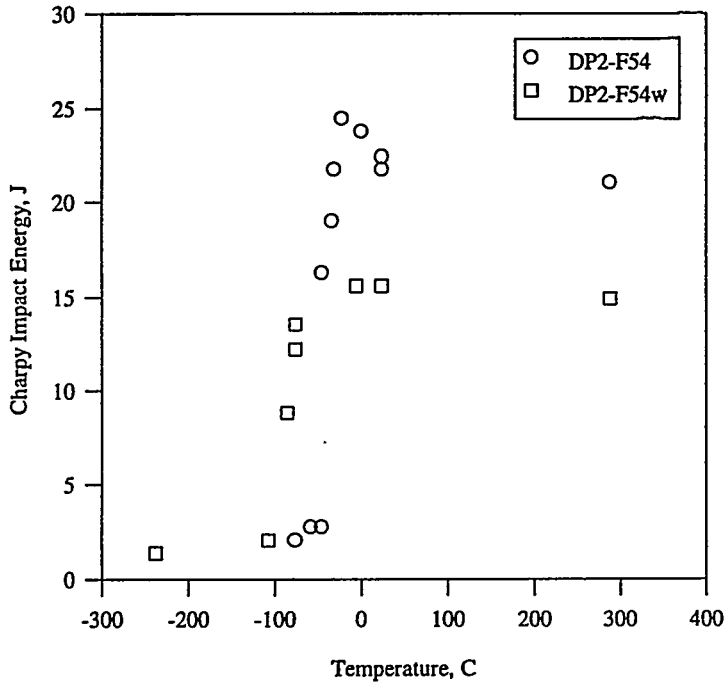

(a) Absorbed energy

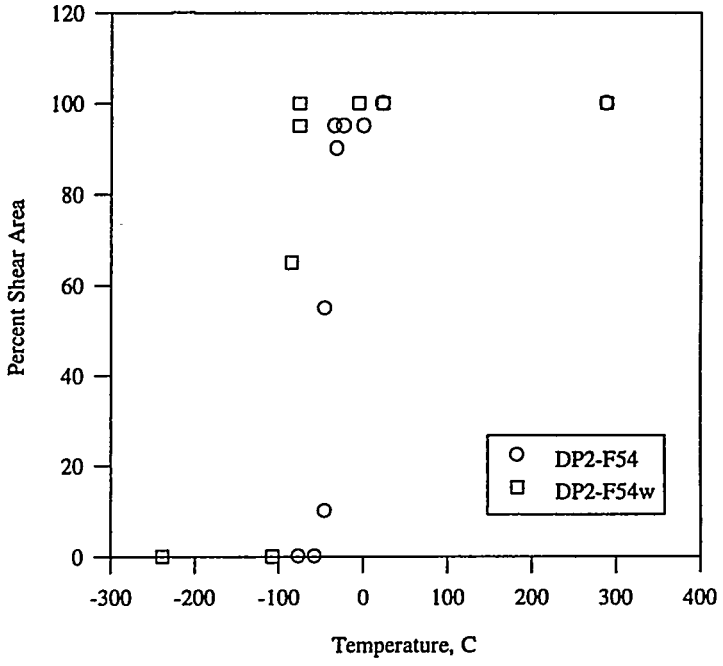

(b) Shear area

Figure 3.16 Charpy data for the MIC pipe base metal and weld metal (L-C oriented, 1/4-thickness specimens)

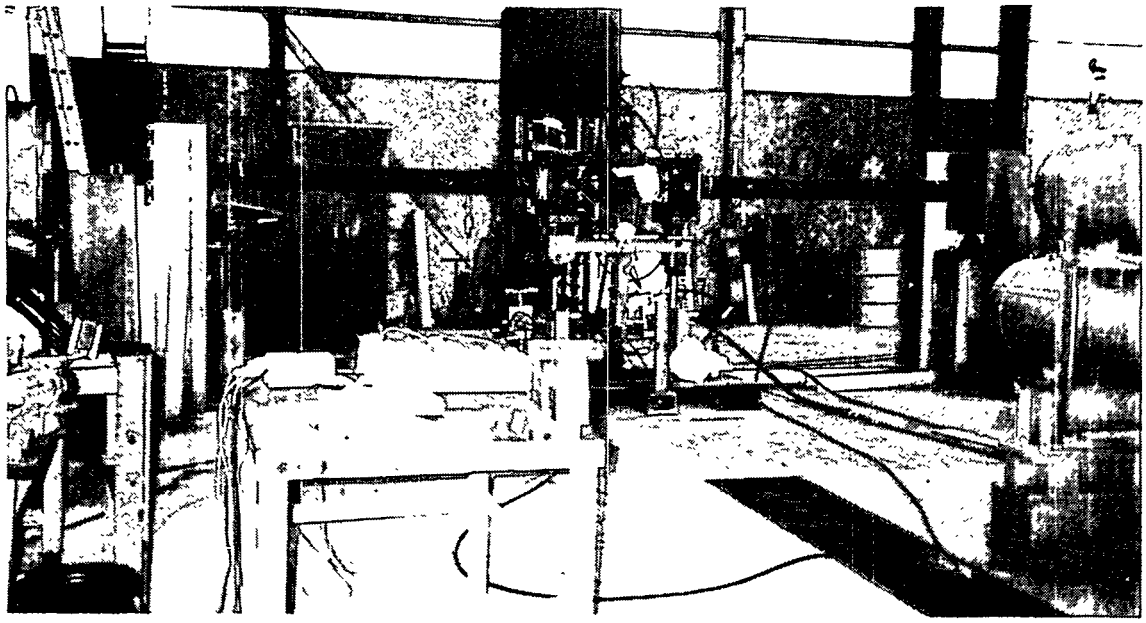

Figure 3.17 Pretest photograph of the MIC pipe test specimen setup in the test frame

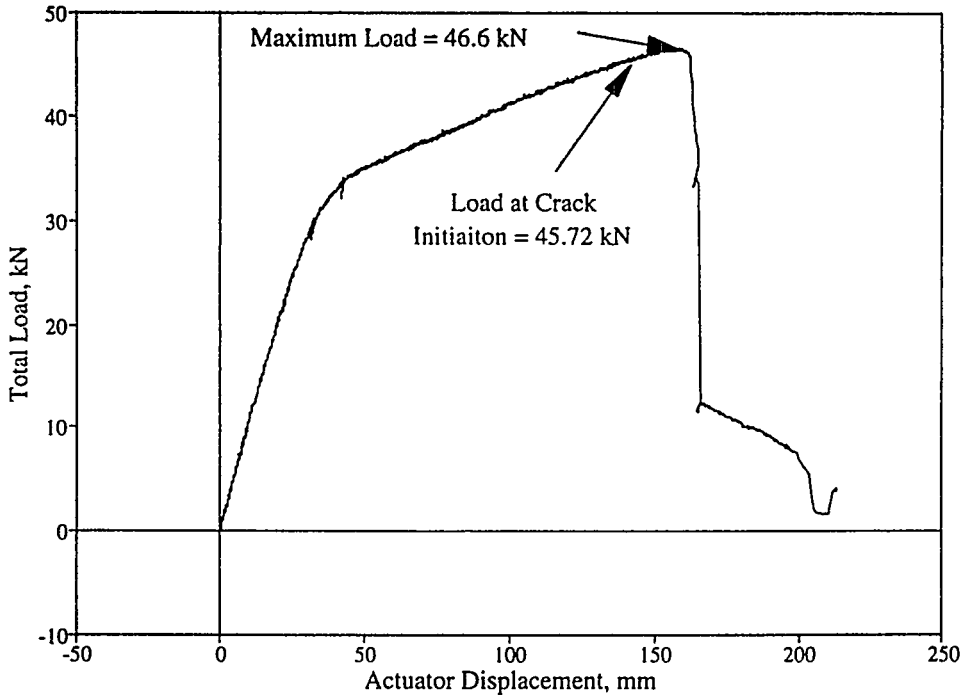

Figure 3.18 Total applied load versus actuator displacement for the Haddam Neck (Connecticut Yankee) Plant MIC experiment

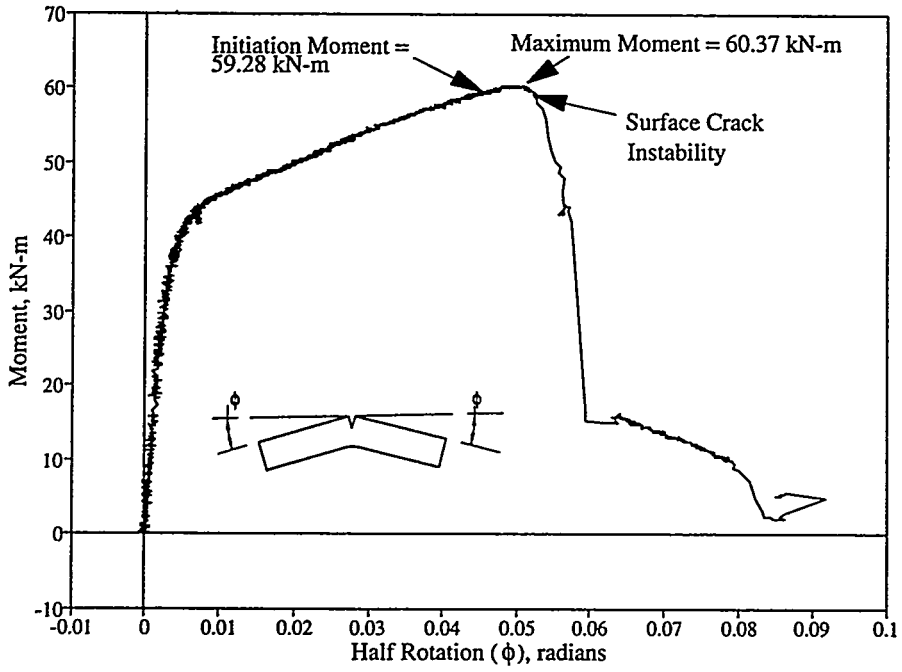

Figure 3.19 Crack section moment versus half rotation (ϕ) for the Haddam Neck (Connecticut Yankee) MIC experiment

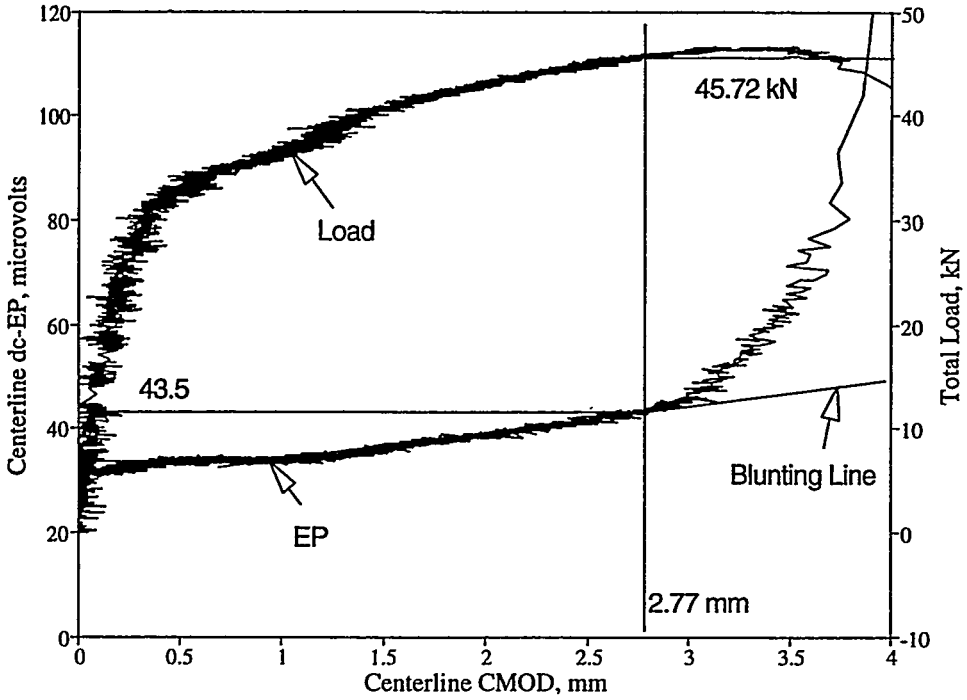

Figure 3.20 Total load and centerline d-c EP versus total centerline CMOD for the Haddam Neck (Connecticut Yankee) Plant MIC experiment

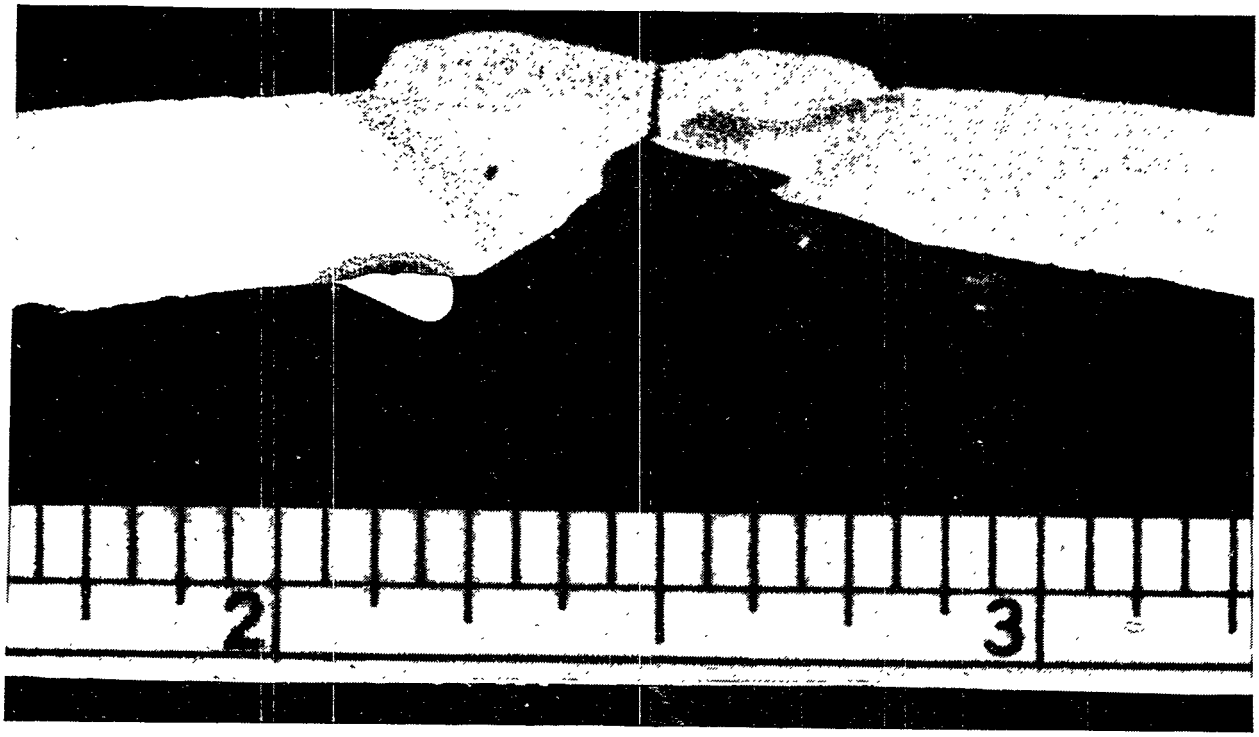

Figure 3.21 Metallographic section of MIC Pipe DP2-F54 (A53 Grade A steel) between Markers 12 and 13 (location of maximum applied stress), scale is in inches

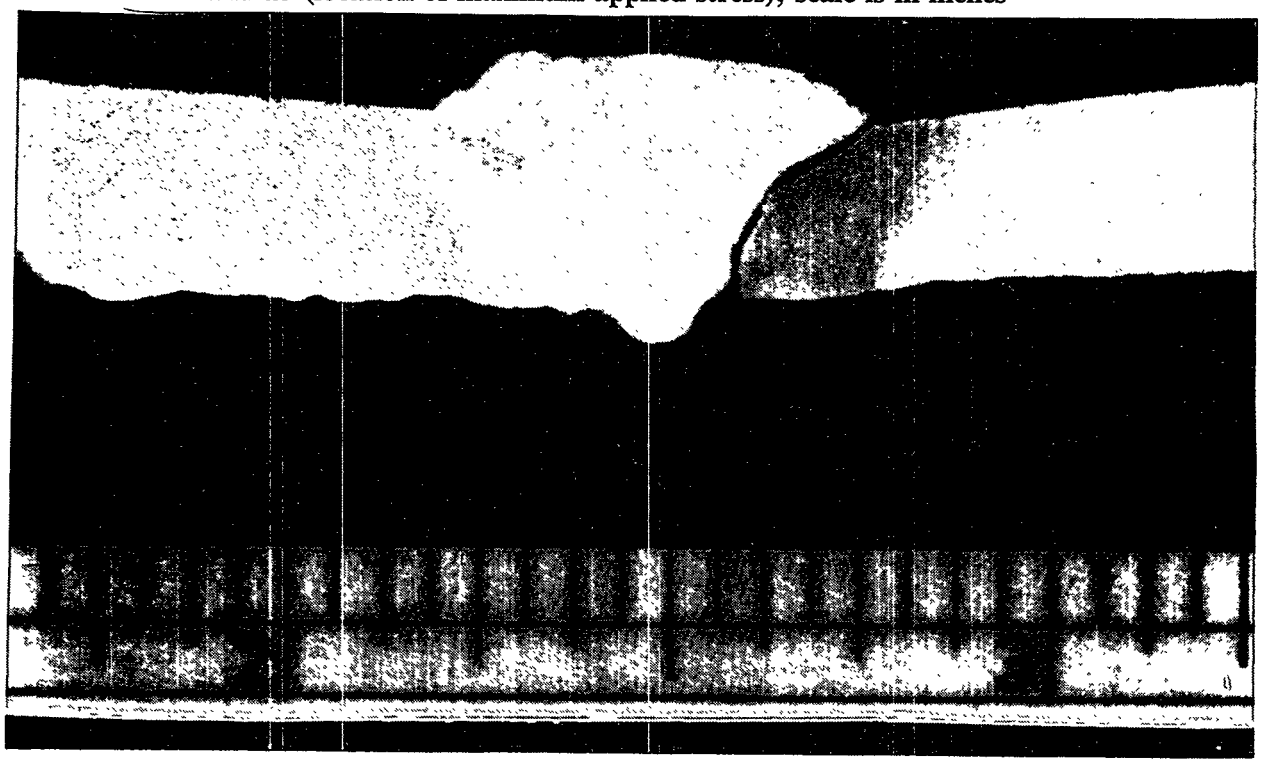

Figure 3.22 Metallographic section of MIC Pipe DP2-F54 (A53 Grade A steel) between Markers 16 and 17 (approximately 75 degrees from the location of maximum stress), scale is in inches

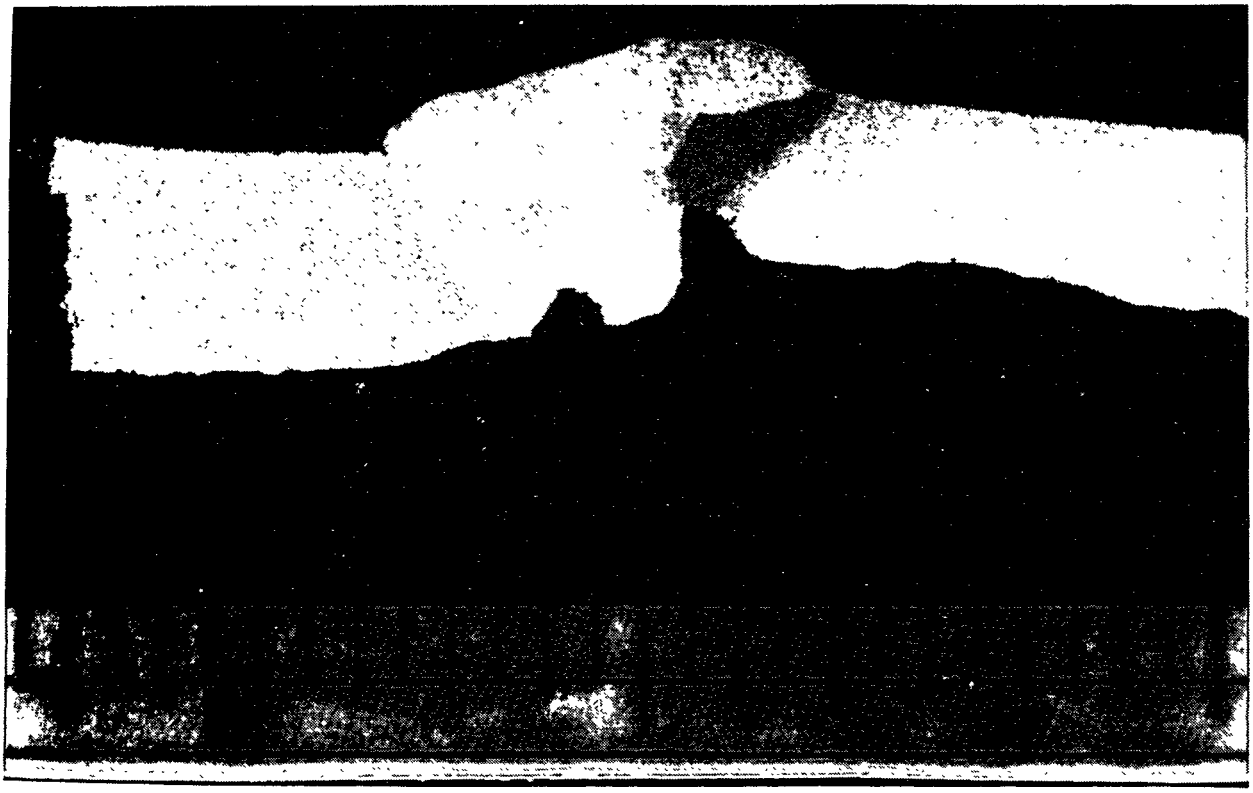

Figure 3.23 Metallographic section of MIC Pipe DP2-F54 (A53 Grade A steel) between Markers 3 and 4, scale is in inches

in inches. The section shown in Figure 3.21 was taken at the deepest flaw location as measured by UT. It is also the location that experienced the maximum stress during the experiment. From Figure 3.21, the corrosion seemed to attack the weld metal more than the flange or pipe base metal; however, some degradation is clearly present in both the pipe and flange material. At this location, the surface crack initiated in the weld metal and grew through the weld thickness.

Figure 3.22 shows a section between Markers 16 and 17, which is approximately 75 degrees from the deepest flaw location. As shown in Figure 3.22, the crack left the weld metal and propagated in the heat-affected zone. At this location, the corrosion seemed to attack the flange and pipe base metal more than the weld metal.

After the experiment, the pipe section was cooled and broken open in order to view the fracture surface. During this procedure, the main crack left its original path and propagated through the flange metal. Figure 3.23 shows a section through this portion of the fracture surface. The left side of the photograph shows the fracture in the flange caused by the main crack propagation. From this figure, the corrosion formed two deep grooves in the weld metal. A closer investigation of these grooves shows many pits and microcracks. It is possible that the sharpness of these microcracks may have been a result of the plasticity compressing blunted regions into sharp crack-like areas. A detailed Energy Dispersion Spectrography study would be required to determine whether these cracks were formed from the corrosion process or blunt cracks closed by mechanical loading. Such a study was beyond the scope of this project.

3.7.4.4 Results of the Analysis Efforts for the Pipe Experiment

In this section, the crack initiation moment and maximum moment from this pipe experiment are compared with predictions of initiation and maximum moment using a number of fracture prediction models. The experimental moment at crack initiation will be compared with predictions from the

SC.TNP1 and SC.TNP2 analysis methods (Ref. 3.8),

SC.ENG1 and SC.ENG2 analysis methods developed during this program and to be published in NUREG/CR-6298, and

R6 Revision 3 Option 1 method (Ref. 3.9).

In addition to the above analysis methods, the maximum experimental moments will be compared with predictions based on the

Net-Section-Collapse (NSC) analysis (Ref. 3.10),

Dimensionless-Plastic-Zone-Parameter (DPZP) analysis (Ref. 3.11), and

ASME Section XI Appendix H and IWB-3650 analysis method (Ref. 3.12).

Details of each of these analysis methods can be found in the appropriate references.

In making predictions for this experiment, quasi-static base metal tensile data (see Table 3.7 and Figure 3.14) and quasi-static weld metal J-R curve data (see Table 3.8 and Figure 3.15) were used. For all of these predictions the flow stress was defined as the average of the yield and ultimate strengths. For the J-estimation schemes, i.e., SC.TNP, SC.ENG, and R6 predictions, the base metal stress-strain curve behavior was modeled using a Ramberg-Osgood relationship where the Ramberg-Osgood equation was fit to the stress-strain data in the range from 0.1-percent strain to the strain corresponding to 80 percent of the ultimate strength. The fit of the stress-strain data to the Ramberg-Osgood equation was made using a Battelle-written computer program, ROFIT. The Ramberg-Osgood coefficients for Specimen F54-t1 (see Table 3.7) were used in these fracture prediction analyses. Figure 3.14 shows the actual base metal tensile data, with the Ramberg-Osgood representation of the data superimposed on the figure.

The J-R curves used in these analyses were based on Deformation theory J-resistance curves, i.e., J_D-R curves. For the small amount of crack growth through the thickness in this surface-crack experiment, the difference between J_M and J_D is insignificant.

A number of different crack size and wall thickness definitions were used in making these predictions, see Table 3.11. Unless otherwise noted, the predictions were based on the optically measured crack size measured after the specimen had been broken open. As can be seen in Figure 3.24, the ultrasonically determined crack depths measured before the experiment were not that different from those measured optically after the experiment. (Note that the optically measured crack depths were measured with respect to the inside surface of the pipe, and not the flange, see Figure 3.35.

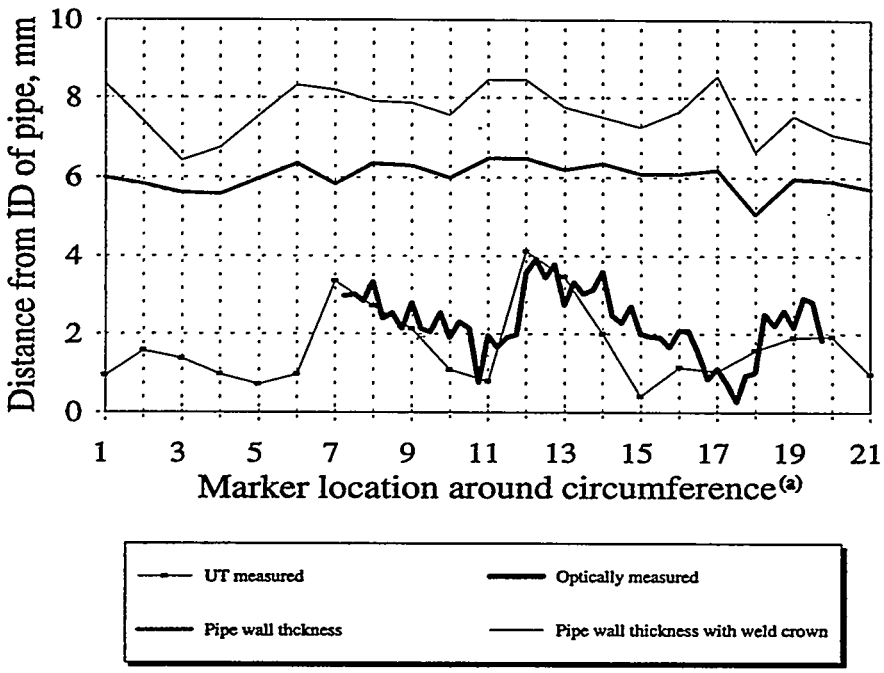

Figure 3.24 Wall thickness and crack depth dimensions for both ultrasonic and optical measurements

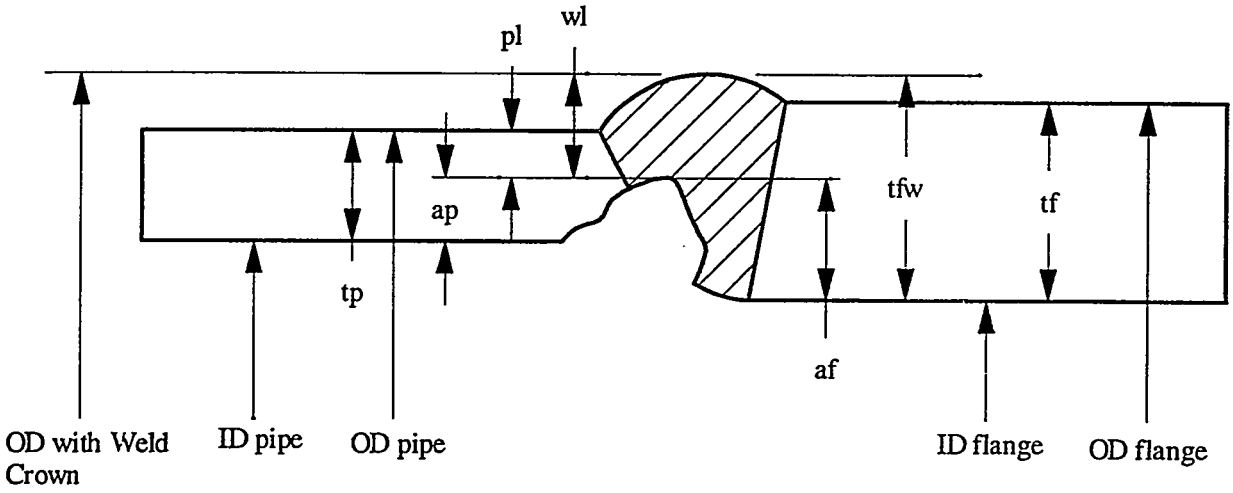

Figure 3.25 Nomenclature used in defining wall thickness and crack depth dimensions, see Table 3.6

Further note that between Locations 20 and 7 around the pipe circumference, no measure of the crack depth was possible using the optical technique since, when the crack was broken open after the test, the fracture did not propagate along the initial weld crack in this region. In this region, the optically measured crack depth was assumed to be equal to the ultrasonically measured crack depth. The wall thickness measurement shown in Table 3.11 for Cases 1 through 4 is the actual measured wall thickness at the crack centerline, without the weld crown, measured posttest using a set of micrometers. The wall thickness measurement in Table 3.11 for Cases 5 through 8 is similar to that for Cases 1 through 4, respectively, except the wall thickness measurement for Cases 5 through 8 includes the height of the weld crown. For each case the crack depth is the depth of the crack at its deepest location. For Cases 1 and 5, the crack length is the total length of the crack, i.e., 360 degrees in both cases. For Cases 2 and 6, the length of the crack is established on an equivalent crack length basis, where the equivalent crack length is defined as the total crack area divided by the maximum crack depth. For Cases 3 and 7, the length of the crack is also established on an equivalent crack length basis. The equivalent crack length in these cases is defined as the area of the crack above the neutral bending axis of the crack section divided by the maximum crack depth, see Figure 3.26. The neutral axis of the crack section was calculated using the optical flaw depth measurements and a computer program (ANSC.EXE) developed at Battelle to conduct Net-Section-Collapse analyses for arbitrarily variable depth circumferential surface cracks.) For Cases 4 and 8, the length of the crack is set at 50 percent of the pipe circumference, which is the same as a 100-percent circumferential length crack in Article IWB-3650 of Section XI of the ASME Code. The final

Table 3.11 Pipe and crack size definitions used in the fracture prediction analyses

Case Number	Wall Thickness Includes Weld Crown Yes/No	Wall Thickness, mm	Crack Size Measured Optically or Ultrasonically	Crack Depth	a_{max}/t[(a)]	Crack Length	$2c/\pi D$
1	No	6.48	Optically	a_{max}	0.605	360°	1.0
2	No	6.48	"	"	0.605	Equivalent[(b)]	0.49
3	No	6.48	"	"	0.605	Equivalent[(c)]	0.359
4	No	6.48	"	"	0.605	180°	0.50
5	Yes	8.12	"	"	0.483	360°	1.0
6	Yes	8.12	"	"	0.483	Equivalent[(b)]	0.49
7	Yes	8.12	"	"	0.483	Equivalent[(c)]	0.346
8	Yes	8.12	"	"	0.483	180°	0.50
9	No	6.48	Ultrasonically	"	0.635	Equivalent[(c)]	0.288

(a) The maximum crack depth measured optically did not occur at one of the locations where a UT assessment of the crack depth was made. The maximum crack depth occurred at a location 6.35 mm (0.25 inch) from Marker Number 12, between Marker Numbers 12 and 13, in Table 3.6, see Figure 3.24.

(b) Total crack area/maximum crack depth.

(c) Crack area above neutral axis/maximum crack depth.

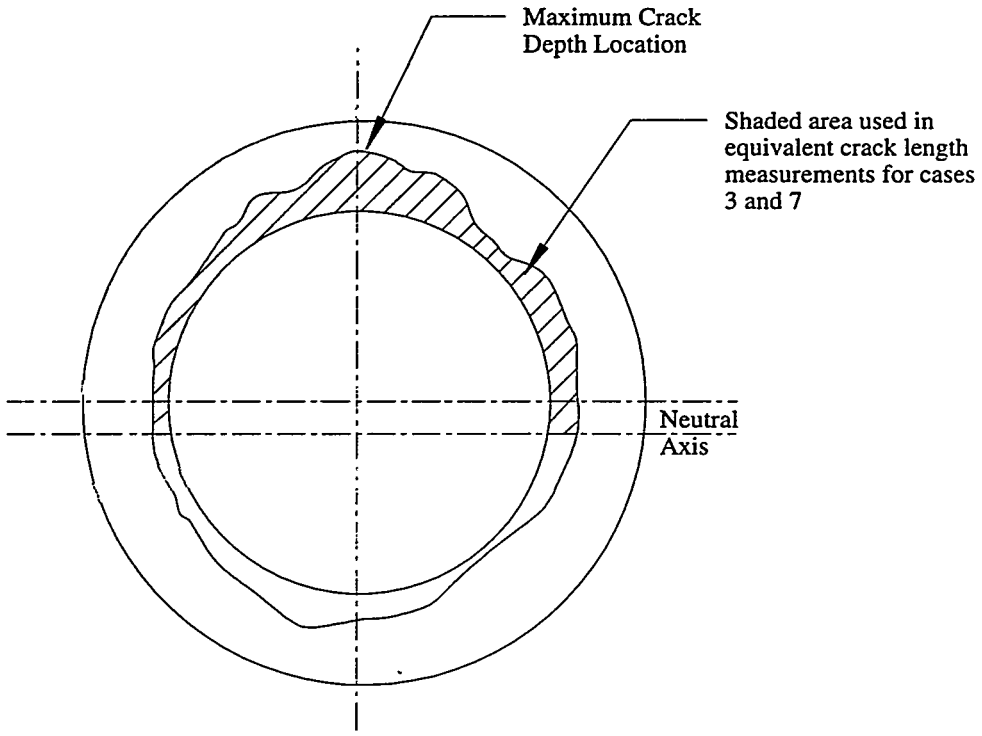

Figure 3.26 Crack areas used in defining equivalent crack lengths for Cases 3 and 7, see Tables 3.11 through 3.13

case shown in Table 3.11 (Case 9) is similar to Case 3 (i.e., maximum crack depth, equivalent crack length using only the area above the neutral bending axis, and wall thickness without weld crown height) except the crack dimensions are based on pretest ultrasonic inspection results instead of the posttest optically measured crack size.

The predictions of the crack initiation moments and the maximum moments using the J-estimation scheme predictions were made with the aid of a Battelle-written computer code, NRCPIPES, Version 2.0. The results of those predictions and the comparisons with the experimental results are shown in Table 3.12 and Table 3.13. Table 3.12 shows the predictions for the crack initiation moments and Table 3.13 shows the results for the maximum moment predictions. For the ASME Appendix H procedure, the safety factor was 1.0 for these calculations.

In examining Tables 3.12 and 3.13, it can be seen that most of the analyses for most of the pipe and flaw geometry definitions underpredicted the experimental crack initiation and maximum moments. The pipe and flaw geometry definition that resulted in the most accurate prediction of the crack initiation and maximum moments is Case 7, i.e., the pipe diameter and wall thickness measurements include the height of the weld crown, and the crack length is an equivalent crack length where the equivalent crack length is the area of the crack above the neutral axis divided by the maximum crack depth. The most inaccurate predictions are for Case 1, in which the pipe diameter and wall thickness measurements do not consider the weld crown and the crack length is assumed to be the maximum depth for 360 degrees, i.e., all the way around the pipe circumference. The agreement between the predictions and the experiment for the most accurate case, i.e., Case 7, is quite good. In fact the

Table 3.12 Predicted initiation moments from analyses of the MIC pipe test[a]

	Initiation Moment, kN-m								
Method	Case 1	Case 2	Case 3	Case 4	Case 5	Case 6	Case 7	Case 8	Case 9
SC.TNP-1	37.79	38.06	41.71	37.86	55.08	53.95	57.26	53.85	43.38
SC.TNP-2	29.17	29.42	32.28	29.26	43.78	42.90	45.56	42.83	33.49
SC.ENG-1	28.45	32.33	37.00	32.06	46.20	49.67	54.86	49.92	38.91
SC.ENG-2	25.77	27.88	30.26	27.75	42.97	45.44	48.58	45.30	30.15
R6 Rev. 3 Opt. 1	31.58	33.12	37.05	32.89	49.93	49.54	53.70	49.33	38.65

(a) Experimental moment at crack initiation = 59.28 kN-m (524.7 in-kips).

Table 3.13 Predicted maximum moments from analyses of the MIC pipe test[a]

	Maximum Moment, kN-m								
Method	Case 1	Case 2	Case 3	Case 4	Case 5	Case 6	Case 7	Case 8	Case 9
NSC	34.72	38.14	43.35	37.84	55.09	57.28	62.53	57.03	46.02
DPZP	33.56	36.86	41.90	36.57	53.20	55.32	60.40	55.07	44.50
SC.TNP-1	38.16	38.63	42.77	38.39	56.87	55.79	60.03	55.65	44.96
SC.TNP-2	29.37	29.79	32.97	29.60	44.90	43.95	47.05	43.86	34.60
SC.ENG-1	28.45	32.47	37.55	32.17	46.67	50.48	56.22	50.20	39.75
SC.ENG-2	25.77	27.88	30.26	27.75	43.23	45.79	49.11	45.64	30.15
R6 Rev. 3 Opt. 1	31.58	33.15	37.35	32.91	50.23	50.00	54.55	49.77	39.21
ASME[b]	20.13	20.30	23.15	20.13	30.74	30.22	33.79	30.74	24.62

(a) Maximum experimental moment = 60.37 kN-m (534.3 in-kips).
(b) Appendix H analysis using Material Category 1 default properties and safety factor of 1.0

predictions of maximum moment using the dimensionless-plastic-zone parameter (DPZP) and the SC.TNP1 analyses for this MIC experiment agree with the experimental results within 0.5 percent. It is also of note from Tables 3.12 and 3.13 that the difference in fracture predictions between the cases, where the crack depth was determined optically (Case 3) and ultrasonically (Case 9), is insignificant, i.e., typically less than 5 percent. This is encouraging in that it showed that in this case the qualified inspection results provided sufficiently accurate information to make good predictions of the moment-carrying capacity of a flawed pipe even for the "real-world" case where the pipe wall and crack dimensions were highly nonuniform.

It is also of note from Table 3.13 that the ASME Appendix H criteria (with a safety factor of 1.0 and using Code default properties) significantly underpredicts the maximum experimental moments for all cases considered. For Case 1 in Table 3.13, the predicted maximum moment was one-third of the experimental value. Finally, in our ASME Appendix H analyses in Table 3.13 all of the results required an EPFM analysis by the screening criterion. A check on LEFM values showed that the allowable LEFM loads were 36 to 57 percent of the EPFM allowable loads, depending on the flaw size dimensions and whether the weld crown was used. Hence, we did not find the LEFM loads to be higher than the EPFM Appendix H loads.

Additional suggested changes to IWB-3650 and Appendix H stemming from the detailed analysis for this experiment are:

- The definition of how far a flaw needs to be from the weld to be considered a base metal flaw needs to be added to IWB-3650, Appendix H and Code Case N-494. These definitions were given in IWB-3640 and Appendix C for austenitic pipe (in Figure IWB-3640-1), but were left out of the ferritic pipe criteria.

- If the pipe is thinner and full-thickness Charpy tests are not possible, there is no guidance on how to treat a subthickness Charpy test for the screening criteria. For example, in the oil and gas industry the equivalent full-thickness Charpy energy is frequently defined as the ratio of the full thickness to the actual specimen thickness times the subthickness Charpy energy.

- The Z-factors are limited to materials with yield strengths of less than 40 ksi. This was originally intended to be for materials with specified minimum yield strengths of less than 40 ksi. There is inconsistent guidance if the actual yield strength is above 40 ksi, i.e., it can be used for limit-load analysis but not for elastic-plastic fracture analysis.

3.7.5 References

3.1 Hiser, A.L., and Callahan, G.M., "A User's Guide to the NRC's Piping Fracture Mechanics Database (PIFRAC)," NUREG/CR-4894, May 1987.

3.2 Scott, P., Olson, R., Wilson, M., and Wilkowski, G., "The Effect of Inertial Loading on Circumferentially Cracked Pipe Results," ASME PVP Vol. 280, June 1994, pp 183-198.

3.3 Scott, P., Olson, R., and Wilkowski, G., "The IPIRG-1 Pipe System Fracture Tests -- Experimental Results," ASME PVP Vol. 280, June 1994, pp 135-152.

3.4 Wilkowski, G.M., and others, "Short Cracks in Piping and Piping Welds," Second semiannual report by Battelle, NUREG/CR-4599, Vol. 1, No. 2, April 1992.

3.5 Kanninen, M.F., Broek, D., Marschall, C.W., Rybicki, E.F., Sampath, S.G., Simonen, F.A., and Wilkowski, G.M., "Mechanical Fracture Predictions for Sensitized Stainless Steel Piping with Circumferential Cracks," Final Report, EPRI NP-192, September 1976.

3.6 1992 ASME Boiler and Pressure Vessel Code, Section III, Division 1, Subsection NB - Class 1 Components, Article NB-3652, July 1, 1992.

3.7 1992 ASME Boiler and Pressure Vessel Code, Section II, Part D - Properties, Table 2B, U, and Y-1, July 1, 1992.

3.8 Scott, P. M., and Ahmad, J., "Experimental and Analytical Assessment of Circumferentially Surface-Cracked Pipes Under Bending," NUREG/CR-4872, BMI-2149, April 1987.

3.9 Milne, I., and others, "Assessment of the Integrity of Structures Containing Defects," Central Electricity Generating Board, UK, R/H/R6 - Rev. 3, May 1986.

3.10 Kanninen, M. F., and others, "Instability Predictions for Circumferentially Cracked Type 304 Stainless Steel Pipes Under Dynamic Loadings," Final Report on EPRI Project T118-2, by Battelle Columbus Laboratories, EPRI Report Number NP-2347, April 1982.

3.11 Wilkowski, G. M., and Scott, P. M., "A Statistical Based Circumferentially Cracked Pipe Fracture Mechanics Analysis for Design or Code Implementation," Nuclear Engineering and Design, 111, pp 173-187, 1989.

3.12 ASME Boiler and Pressure Vessel Code, Section XI, Appendix H, American Society of Mechanical Engineers, 1992.

NRC FORM 335 (2-89) NRCM 1102, 3201, 3202

U.S. NUCLEAR REGULATORY COMMISSION

BIBLIOGRAPHIC DATA SHEET

(See instructions on the reverse)

1. REPORT NUMBER (Assigned by NRC. Add Vol., Supp., Rev., and Addendum Numbers, if any.)

NUREG/CR-4599
BMI-2173
Vol. 4, No. 1

2. TITLE AND SUBTITLE

Short Cracks in Piping and Piping Welds
Seventh Program Report
March 1993 - December 1994

3. DATE REPORT PUBLISHED

MONTH	YEAR
April	1995

4. FIN OR GRANT NUMBER

B5702

5. AUTHOR(S)

G. Wilkowski, N. Ghadiali, D. Rudland, P. Krishnaswamy, S. Rahman, P. Scott

6. TYPE OF REPORT

Technical

7. PERIOD COVERED *(Inclusive Dates)*

3/93 - 12/94

8. PERFORMING ORGANIZATION – NAME AND ADDRESS *(If NRC, provide Division, Office or Region, U.S. Nuclear Regulatory Commission, and mailing address; if contractor, provide name and mailing address.)*

Battelle
505 King Avenue
Columbus, OH 43201

9. SPONSORING ORGANIZATION – NAME AND ADDRESS *(If NRC, type "Same as above"; if contractor, provide NRC Division, Office or Region, U.S. Nuclear Regulatory Commission, and mailing address.)*

Division of Engineering Technology
Office of Nuclear Regulatory Research
U.S. Nuclear Regulatory Commission
Washington, D.C. 20555

10. SUPPLEMENTARY NOTES

11. ABSTRACT *(200 words or less)*

This is the seventh progress report of the U.S. Nuclear Regulatory Commission's research program entitled "Short Cracks in Piping and Piping Welds". The program objective is to verify and improve fracture analyses for circumferentially cracked large-diameter nuclear piping with crack sizes typically used in leak-before-break (LBB) analyses and in-service flaw evaluations. All work in the eight technical tasks have been completed. Ten topical reports are scheduled to be published. Progress only during the reporting period, March 1993 - December 1994, not covered in the topical reports is presented in this report. Details about the following efforts are covered in this report: Improvements to the two computer programs NRCPIPE and NRCPIPES to assess the failure behavior of circumferential through-wall and surface-cracked pipe, respectively; Pipe material property database PIFRAC; Circumferentially cracked pipe database CIRCUMCK.WK1; An assessment of the proposed ASME Section III design stress rule changes on pipe flaw tolerance; and A pipe fracture experiment on a section of pipe removed from service degraded by microbiologically induced corrosion (MIC) which contained a girth weld crack. Progress in the other tasks is not repeated here as it has been covered in great detail in the topical reports.

12. KEY WORDS/DESCRIPTORS *(List words or phrases that will assist researchers in locating the report.)*

Fracture, pipe, J-R curve, J-integral, NRCPIPE Code, pipe stress analysis, microbiologically induced corrosion, PIFRAC, CIRCUMCK

13. AVAILABILITY STATEMENT

Unlimited

14. SECURITY CLASSIFICATION

(This Page)

Unclassified

(This Report)

Unclassified

15. NUMBER OF PAGES

16. PRICE